

Supporting Information

Organic and Biomolecular Chemistry

Enhanced Ion Binding by the Benzocrown Receptor and a Carbonyl of the Aminonaphthalimide Fluorophore in Water- Soluble Logic Gates

Andreas Diacono, Marie Claire Aquilina, Andrej Calleja, Godfrey Agius,
Gabriel Gauci, Konrad Szaciłowski and David C. Magri*

Department of Chemistry, Faculty of Science
University of Malta, Msida, Malta, MSD 2080
email: david.magri@um.edu.mt
Phone: (+356) 2340 2276

Table of Contents

Experimental	2
Fluorescence Quantum Yields	3
Fig. S37 UV-visible absorption spectra of 1 before (blue) and after (red) extracting from water into octan-1-ol. Measurement based on peak at 390 nm.....	4
Fig. S38 UV-visible absorption spectra of 2 before (blue) and after (red) extracting from water into octan-1-ol. Measurements based on peak at 390 nm.....	4
Fig. S39 UV-visible absorption spectra (a) 14 μM of 1 with Na^+ , (b) 16 μM of 2 with Na^+ , (c) 14 μM of 1 with K^+ , (d) 22 μM of 2 with K^+ at 10^{-4} M or 10^{-9} M H^+ concentrations.....	5
Fig. S40 UV-visible absorbance spectra of (a) 1 between pH 2-11, (b) 2 between pH 2-11, (c) Fluorescence emission spectra of 1 between pH 2-11, (d) Fluorescence emission spectra of 2 between pH 2-11, (e) Fluorescence intensity of 1 plotted against pH, (f) Fluorescence intensity of 2 plotted against pH in water. λ_{ex} used were 412 nm and 408 nm for 1 and 2 , respectively.....	6
Fig. S41 Fluorescence emission spectra of (a) 14 μM 1 with Na^+ , (b) 16 μM 2 with Na^+ , (c) 14 μM 1 with K^+ , (d) 22 μM 2 with K^+ . The λ_{ex} used were 390 nm and 400 nm at pH 4 and pH 9, respectively. The anion is Cl^-	7
Table S1 Truth table for logic gate 2 in 1:1 (v/v) methanol/water and water.....	7
Fig. S1-S9 ^1H NMR spectra of 1-9 in $\text{CDCl}_3/0.03\%$ TMS.....	8-16
Fig. S10-S18 ^{13}C NMR spectra of 1-9 in $\text{CDCl}_3/0.03\%$ TMS.....	17-25
Fig. S19-S27 FTIR spectra of 1-9 (KBr Disc).....	26-34
Fig. S28-S36 HRMS of 1-9	35-43

Experimental

4-Aminobenzo-18-crown-6 (98%, Fluka), 4-aminobenzo-15-crown-5 (97%, Sigma-Aldrich), 3,4-dimethoxyaniline (>98%, TCI), 4-chloro-1,8-naphthalic anhydride (94%, Alfa Aesar), 4-bromo-1,8-naphthalic anhydride (95%, Sigma-Aldrich), methylpiperazine (98%, Alfa-Aesar), methanol (99.9%, Carlo Erba), dichloromethane (99.9%, Carlo Erba), 2-methoxyethanol (99.5%, Carlo Erba), glacial acetic acid (99.8%, Sigma-Aldrich), N,N-dimethylformamide (HPLC, Sigma-Aldrich), tetrabutylammonium hydroxide solution (1.5 M in 40% water, Fluka Analytical), octan-1-ol (GPR, Fisher) (1,4-dioxane (99%, Fischer Scientific), sodium hydroxide pellets (>98%, Fluka) aluminium oxide (Fluka) and chloroform-*d* (99.8%, 0.03% tetramethylsilane (TMS), Carlo Erba), sodium chloride (ARG, Fisher), potassium chloride (ARG, Labkem).

Syntheses were performed in Quickfit® round-bottom flasks with an IKA C-MAG HS 7 hot plate assisted by an IKA ETS-D5 temperature probe to help maintain a constant temperature during reflux. TLC aluminium foils (silica gel coated with fluorescent indicator 254 nm, Fluka analytical) were used for thin-layer chromatography using homemade capillary tubes. The spots were observed under long wavelength (365 nm) and short wavelength (254 nm) UV light from a UVGL-58 handheld lamp. Melting points were measured with a Stuart SMP11 melting point apparatus.

NMR spectra were acquired with a Bruker Avance III HD NMR spectrometer fitted with an Ascend 500 11.75 Tesla superconducting magnet and a multinuclear 5mm PABBO probe. The frequencies are 500.13 MHz for ¹H NMR and 125.76 MHz for ¹³C NMR, respectively. Data were analysed and processed with Topspin version 4.0.5. Chemical shifts were reported in ppm downfield with respect to TMS at 0.00 ppm at 298 K. Data for ¹H are reported with multiplicity (s = singlet, d = doublet, t = triplet, m = multiplet). Infra-red spectra were recorded using a Shimadzu IR-Affinity-1 spectrophotometer between 4000-400 cm⁻¹ as KBr disks or as a thin film between NaCl plates. The instrument was calibrated against 1601 cm⁻¹ polystyrene absorption peak. The high resolution mass spectrometry (HRMS) was performed by ESI-ToF outsourced to Medac Ltd (UK). <http://medacltd.com/>

Ultraviolet-visible absorption spectroscopy data was obtained with a dual beamed Jasco V-650 spectrophotometer and processed with Spectra Manager V.2.0. Spectra were recorded at 0.5 nm data intervals and a scan rate of 400 nm min⁻¹. The fluorescence spectra were acquired with a Jasco FP-8300 spectrophotometer and processed with the same version of Spectra Manager. Quartz SUPRASIL cuvettes (101-10-40) with 10 mm pathlength with transparent windows on all four sides were used. The excitation wavelengths were ideally the isosbestic point. The parameters for the data acquisition were data intervals of 1.0 nm, excitation bandwidth of 1.0 nm, emission bandwidth of 2.5 nm, scan rate of 500 nm min⁻¹ with the sensitivity response set on high. The pH was monitored using a HANNA pH 210 Microprocessor pH meter. The pH meter was calibrated with buffer solutions at pH 7.0 and 4.0.

Fluorescence Quantum Yields

The fluorescence quantum yields (Φ_f) were determined in 1:1 (v/v) methanol/water and water using quinine hemisulfate monohydrate in 0.1 M H₂SO₄ in water as the standard ($\Phi_f = 0.58$). Measurements of **1-3** were performed at pH 4 and pH 9 in the presence and absence of alkaline salts using the equation:

$$\Phi_f = Q_{STD} \times \frac{I}{I_{STD}} \times \frac{OD_{STD}}{OD} \times \frac{n^2}{n_{STD}^2}$$

where Q_{STD} is the fluorescence quantum yield of standard, I is the emission area of sample, I_{STD} is the emission area of standard, OD is the optical density and n is the solvent refractive index.

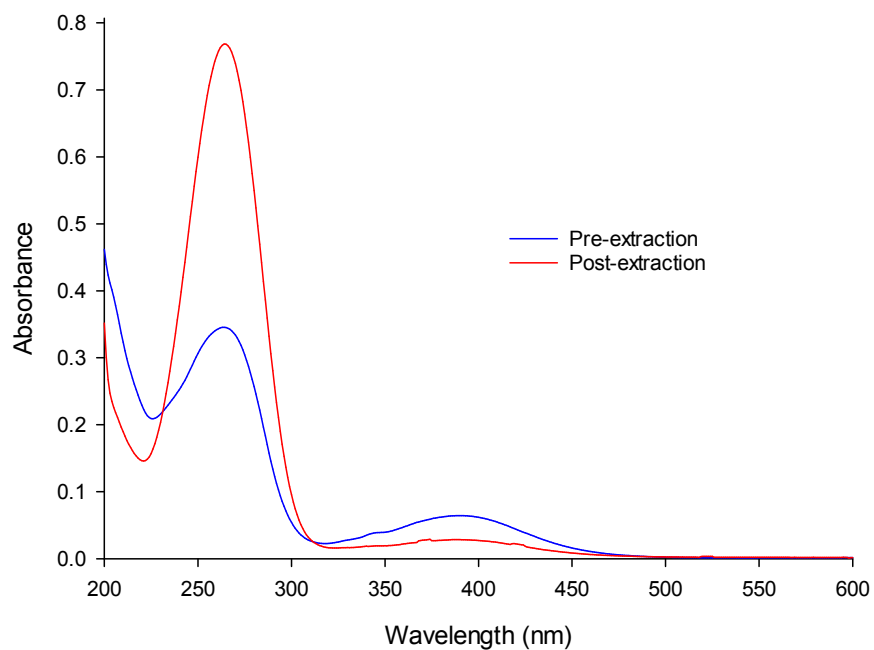


Fig. S37 UV-visible absorption spectra of **1** before (blue) and after (red) extracting from water into octan-1-ol. Measurement based on peak at 390 nm.

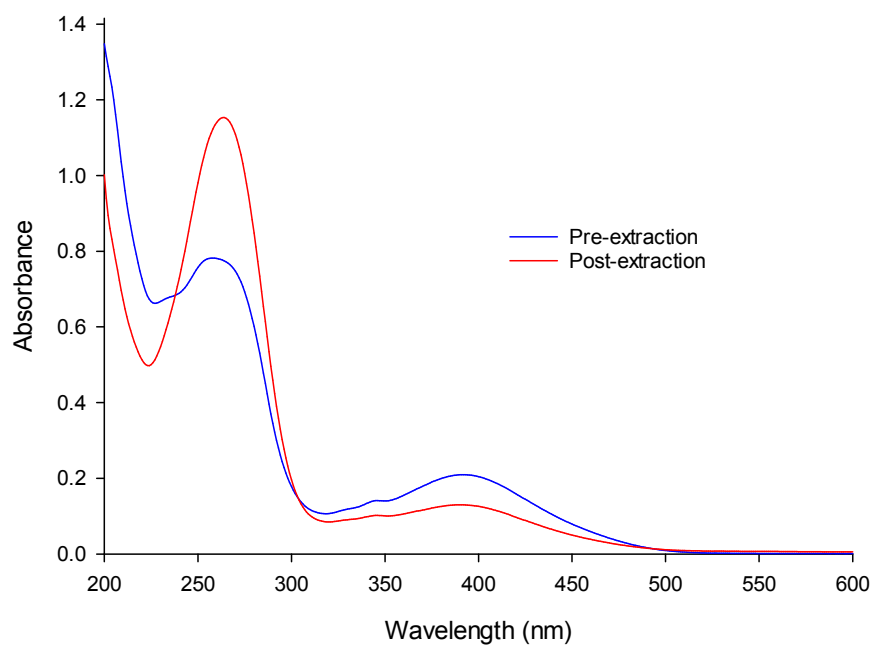


Fig. S38 UV-visible absorption spectra of **2** before (blue) and after (red) extracting from water into octan-1-ol. Measurements based on peak at 390 nm.

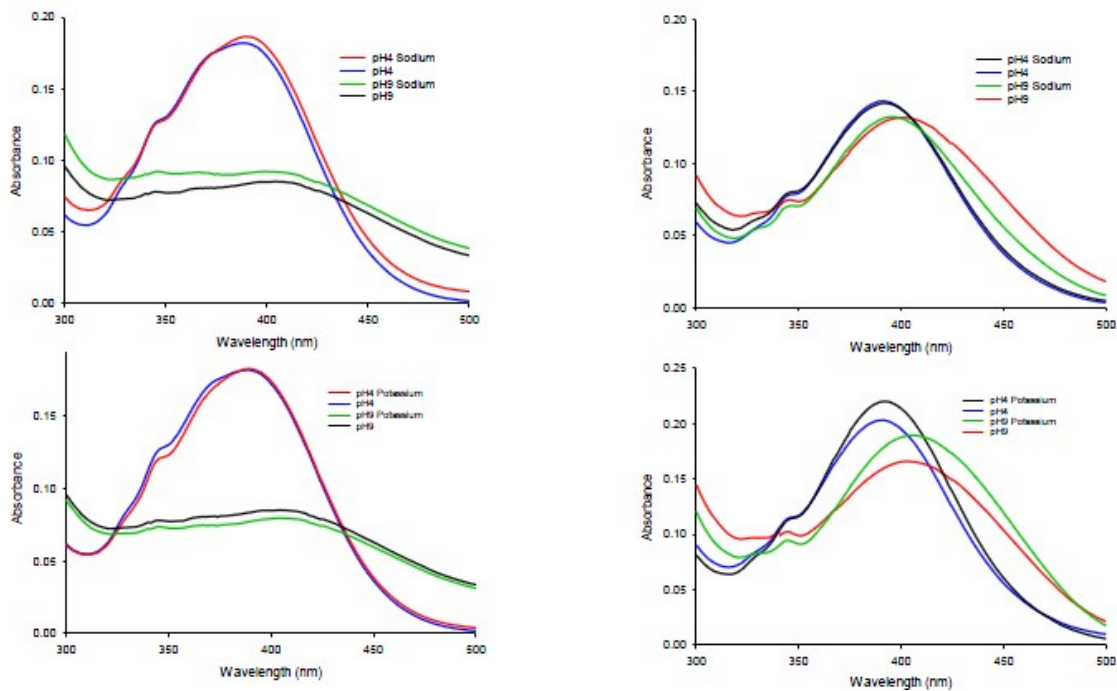


Fig. S39 UV-visible absorption spectra (a) 14 μM of **1** with Na^+ , (b) 16 μM of **2** with Na^+ , (c) 14 μM of **1** with K^+ , (d) 22 μM of **2** with K^+ at 10^{-4} M or 10^{-9} M H^+ concentrations.

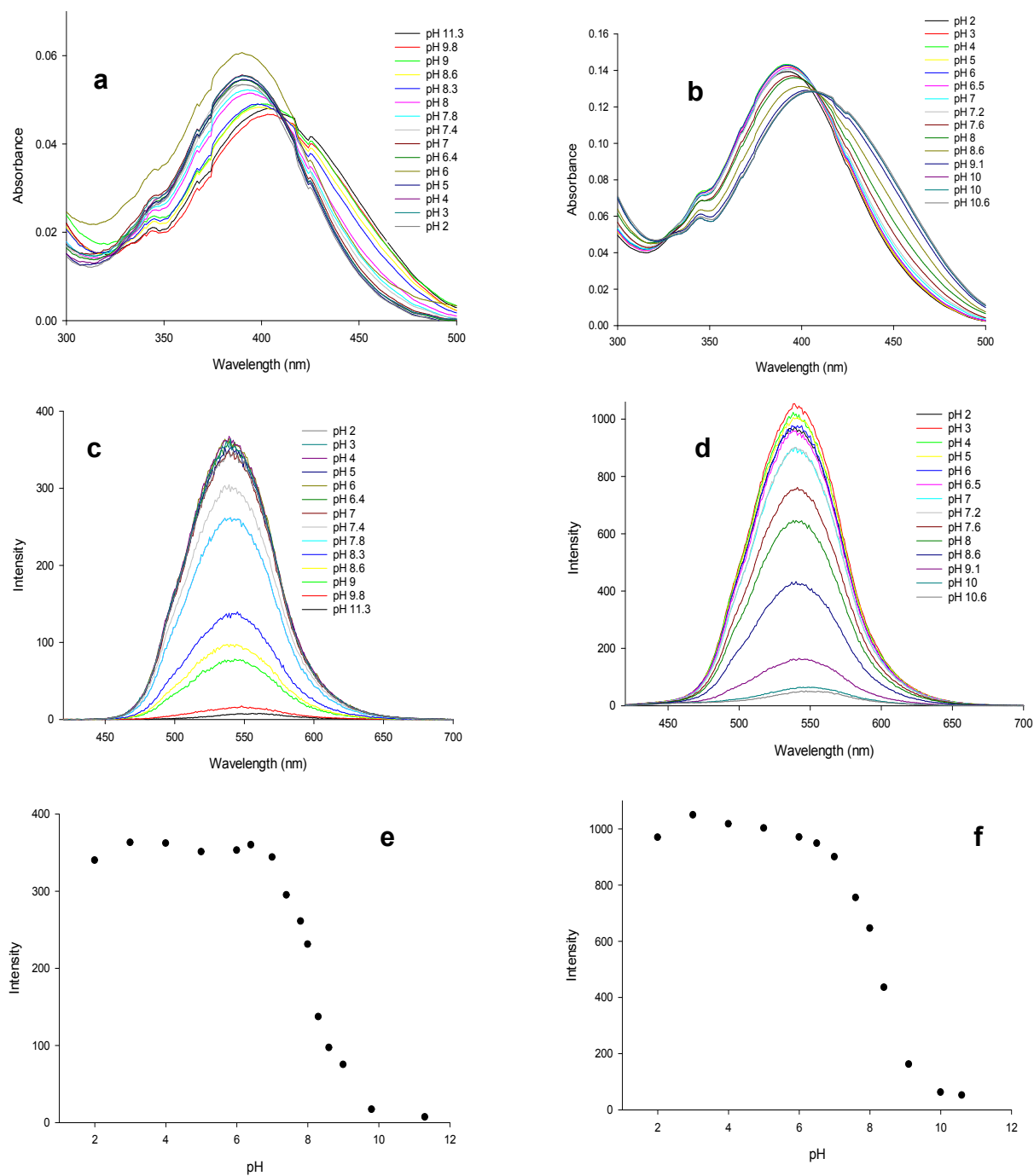


Fig. S40 UV-visible absorbance spectra of (a) **1** between pH 2-11, (b) **2** between pH 2-11, (c) Fluorescence emission spectra of **1** between pH 2-11, (d) Fluorescence emission spectra of **2** between pH 2-11, (e) Fluorescence intensity of **1** plotted against pH, (f) Fluorescence intensity of **2** plotted against pH in water. λ_{ex} used were 412 nm and 408 nm for **1** and **2**, respectively.

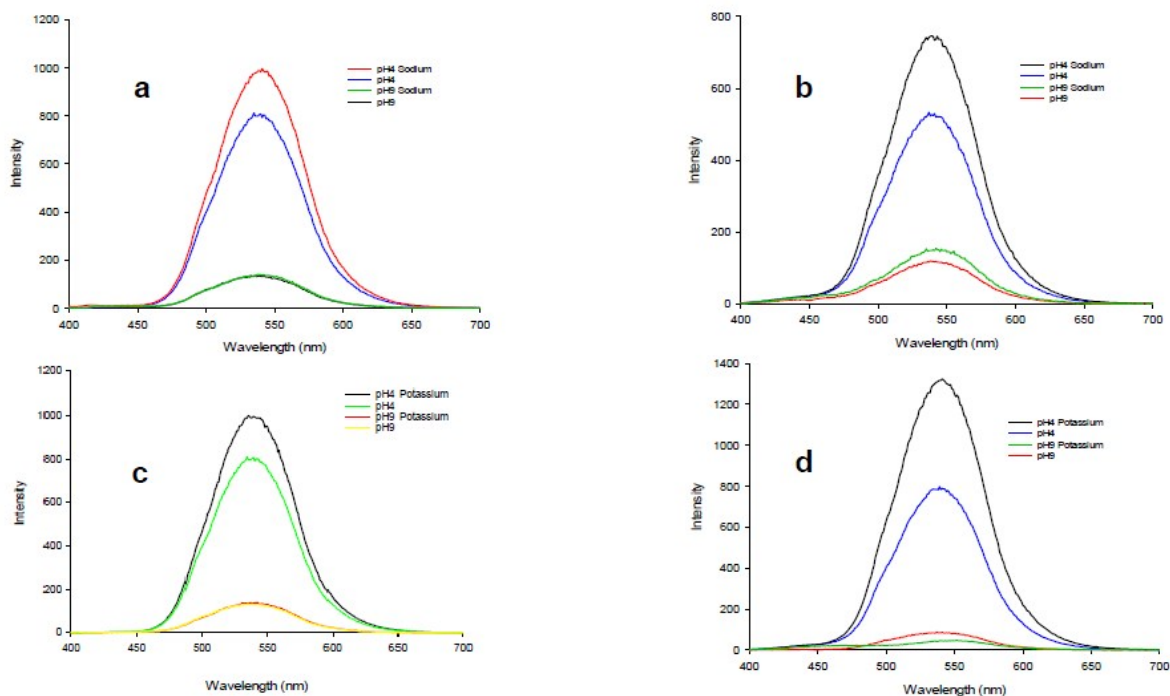


Fig. S41 Fluorescence emission spectra of (a) 14 μM **1** with Na^+ , (b) 16 μM **2** with Na^+ , (c) 14 μM **1** with K^+ , (d) 22 μM **2** with K^+ . The λ_{ex} used were 390 nm and 400 nm at pH 4 and pH 9, respectively. The anion is Cl^- .

Table S1 Truth table for logic gate **2** in 1:1 (v/v) methanol/water and water.^a

Input ₁ (H^+) ^b	Input ₂ (K^+) ^c	Output $\Phi_{\text{F}}^{\text{d}}$ MeOH/ H_2O	Output $\Phi_{\text{F}}^{\text{d}}$ H_2O
0 (low)	0 (low)	0 (low, 0.008)	0 (low, 0.014)
0 (low)	1 (high)	0 (low, 0.038)	0 (low, 0.015)
1 (high)	0 (low)	0 (low, 0.055)	1 (high, 0.17)
1 (high)	1 (high)	1 (high, 0.28)	1 (high, 0.26)

^a 8 μM **2** excited at 400 nm. ^b High H^+ level 10^{-4} M. Low H^+ level 10^{-9} M. Addition of 0.10 M HCl or 0.10 M Bu_4NOH solution (25% wt. in H_2O) ^c High K^+ level 200 mM KCl. Low Na^+ level no KCl added. ^d Quantum yields measured with reference to quinine sulfate in 0.1 M H_2SO_4 water.

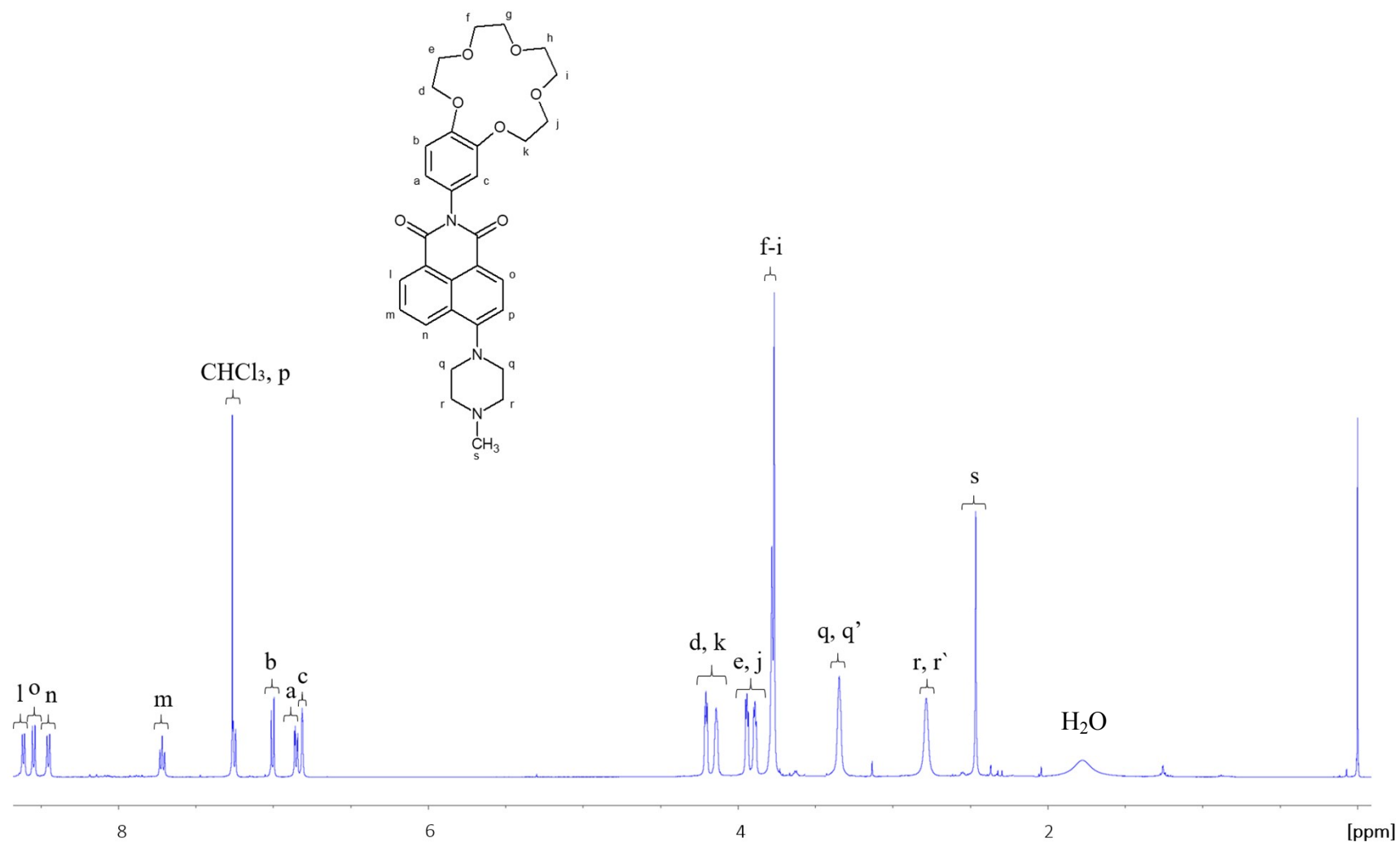


Figure S1. ^1H NMR spectrum of **1** in $\text{CDCl}_3/0.03\%$ TMS.

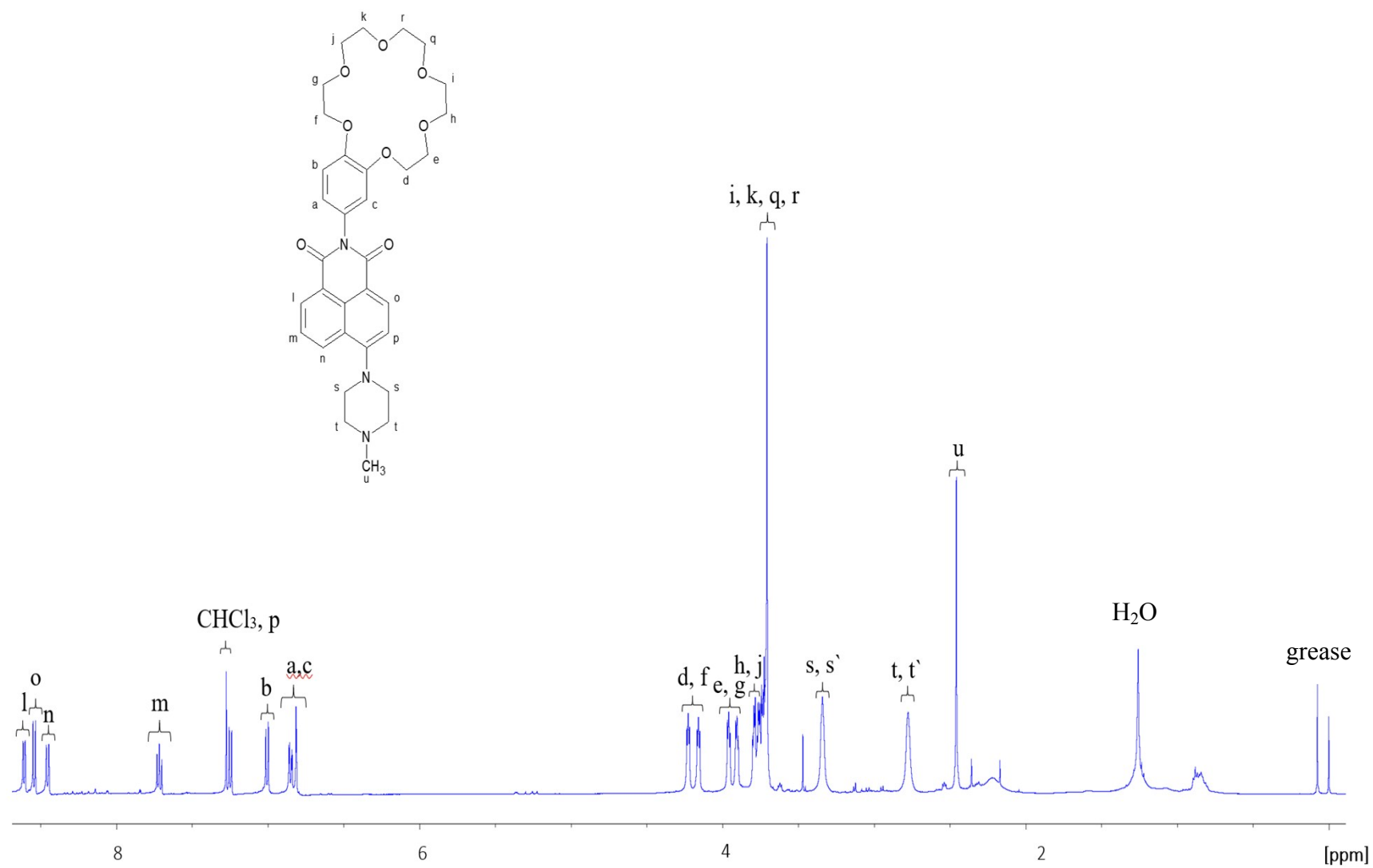


Figure S2. ¹H NMR spectrum of **2** in CDCl₃/0.03% TMS.

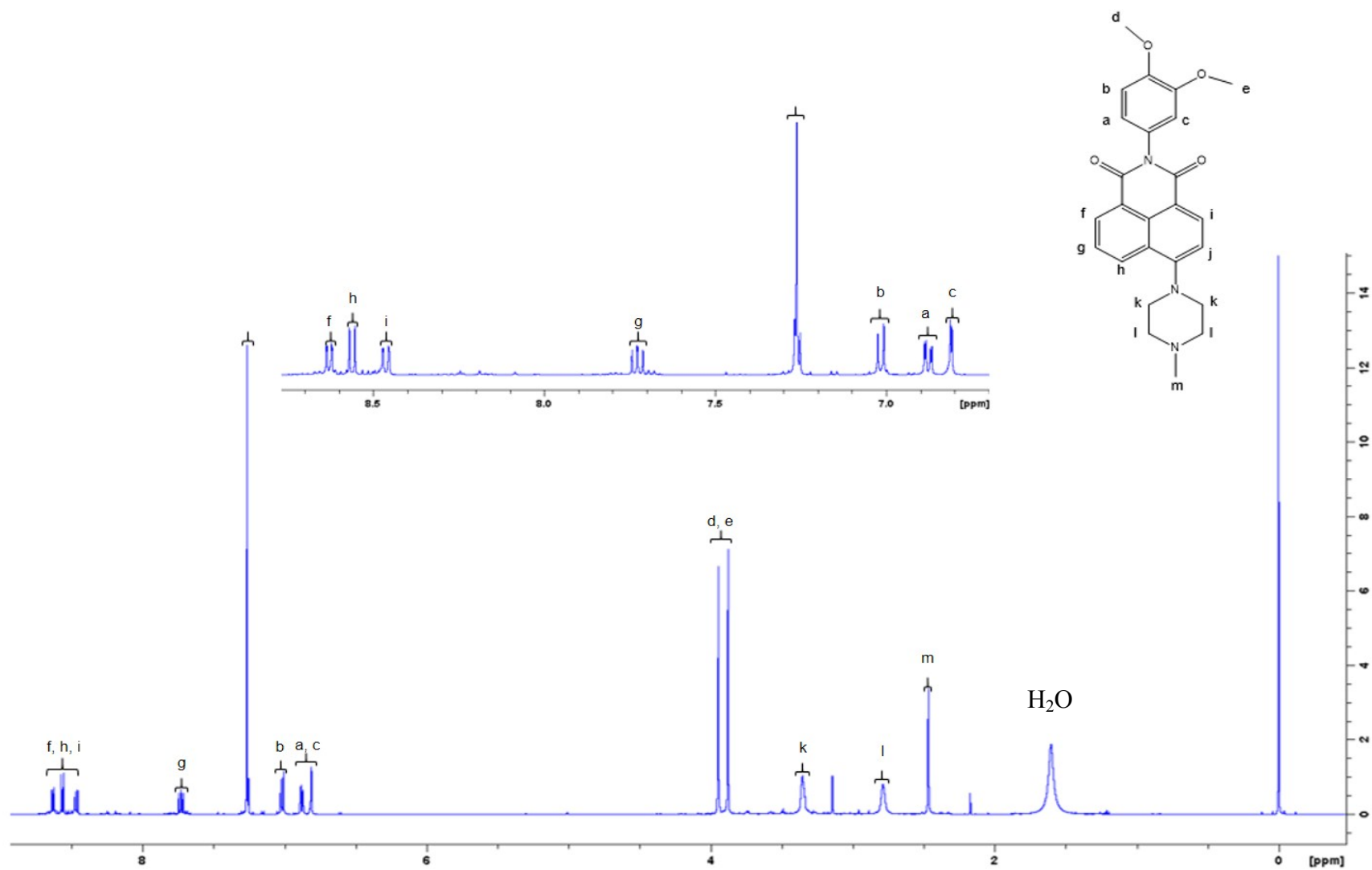


Figure S3. ^1H NMR spectrum of **3** in $\text{CDCl}_3/0.03\%$ TMS.

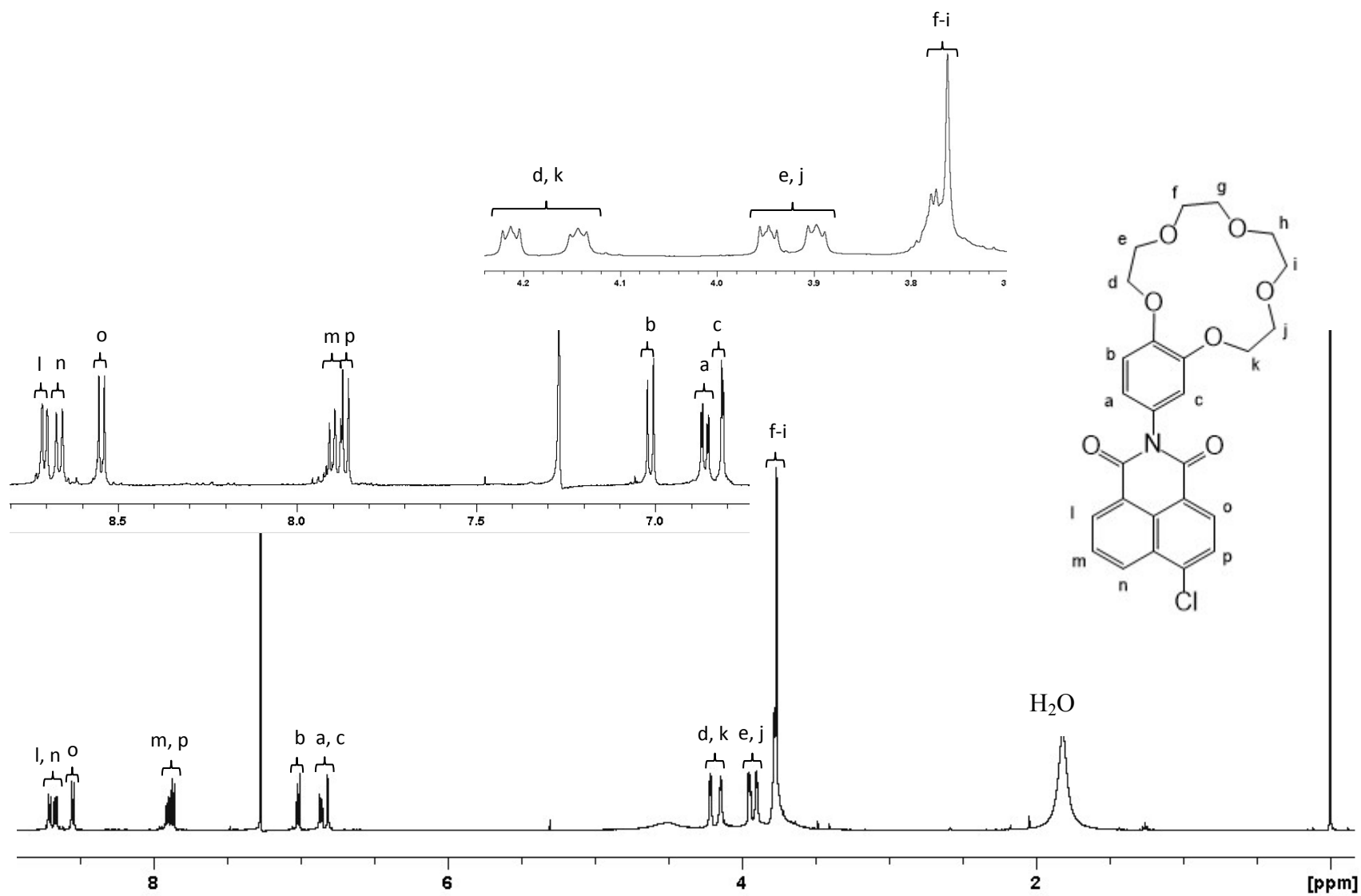


Figure S4. ¹H NMR spectrum of **4** in CDCl₃/TMS.

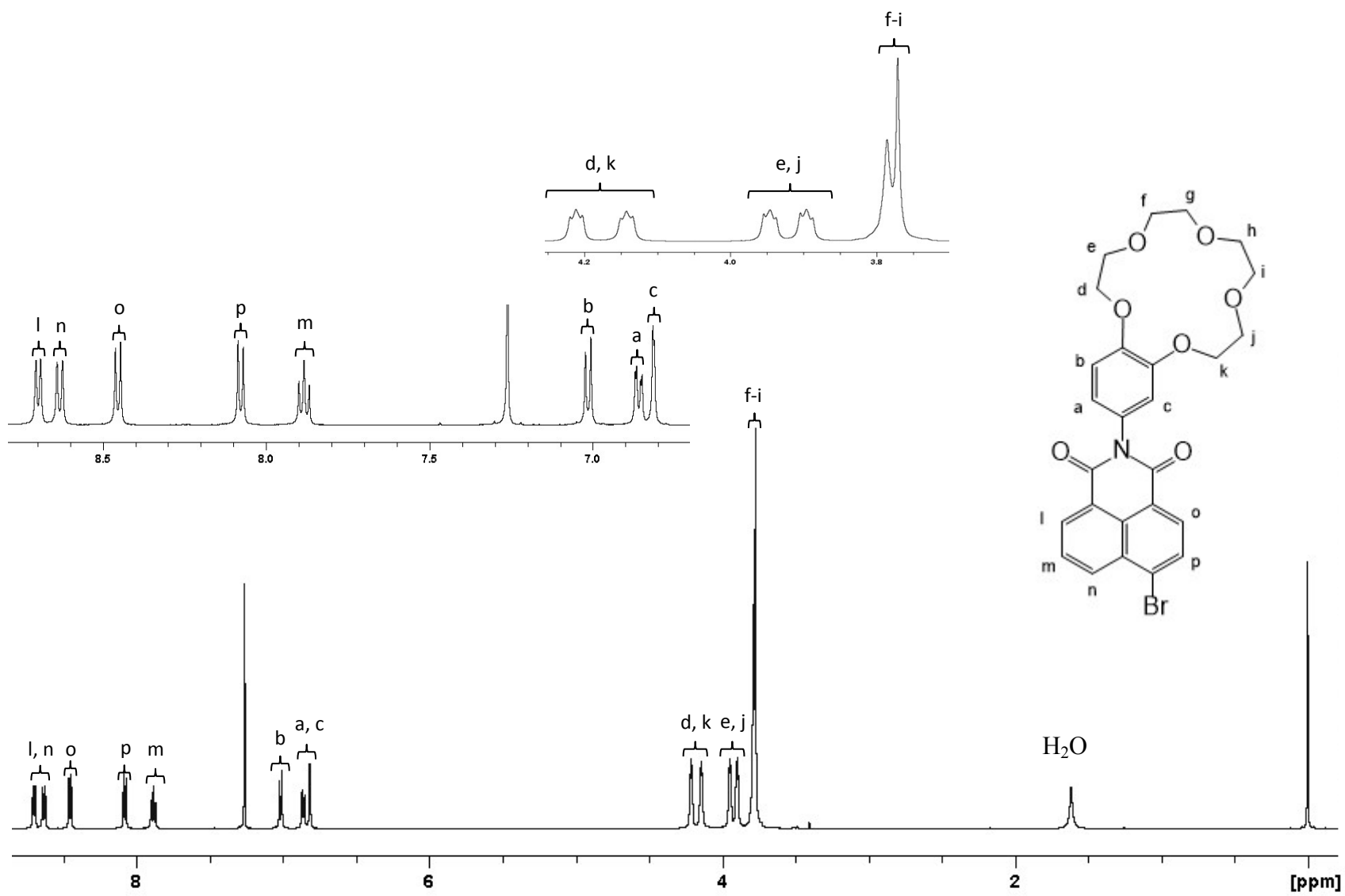


Figure S5. ^1H NMR spectrum of **5** in CDCl_3/TMS .

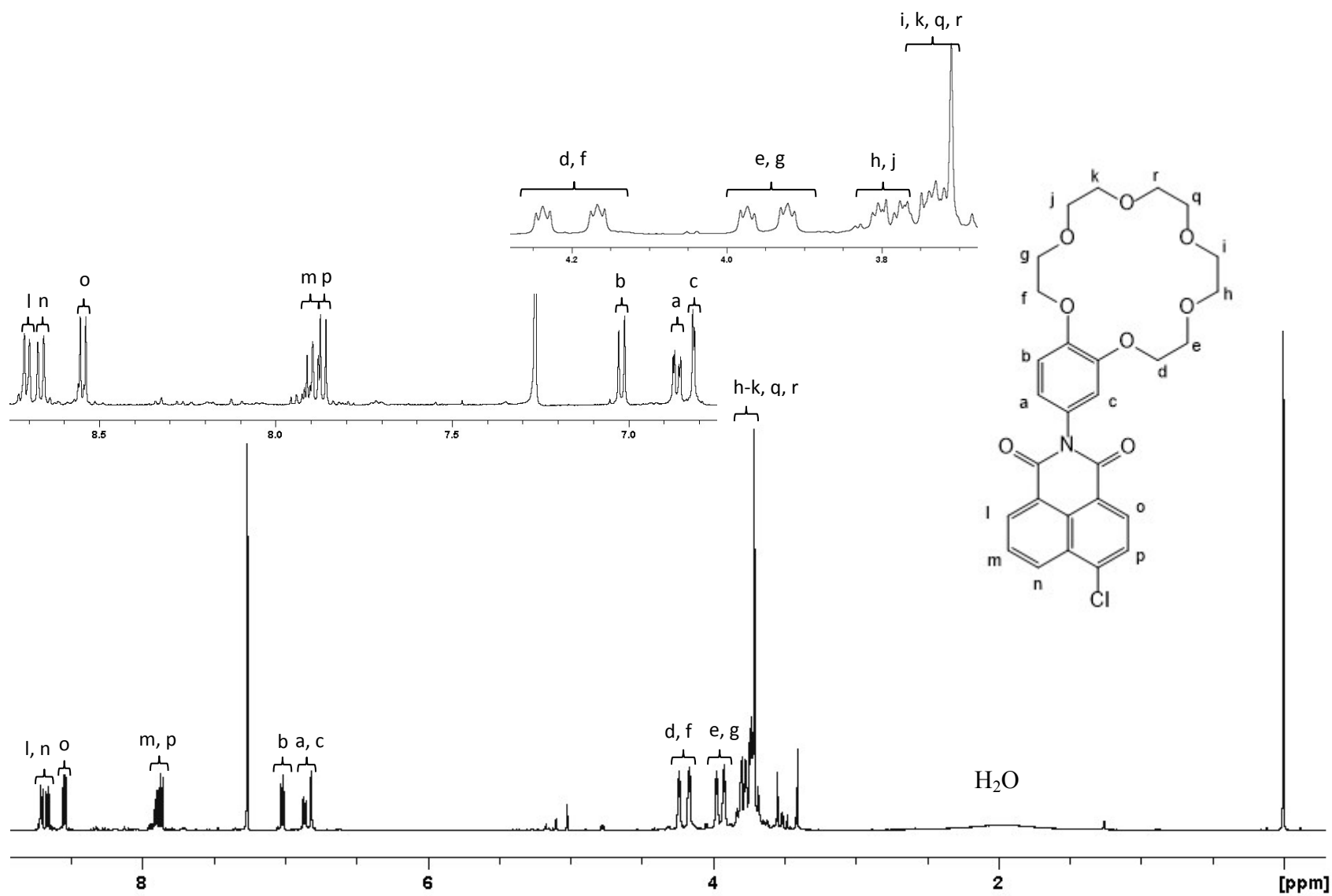


Figure S6. ^1H NMR spectrum of **6** in CDCl_3/TMS .

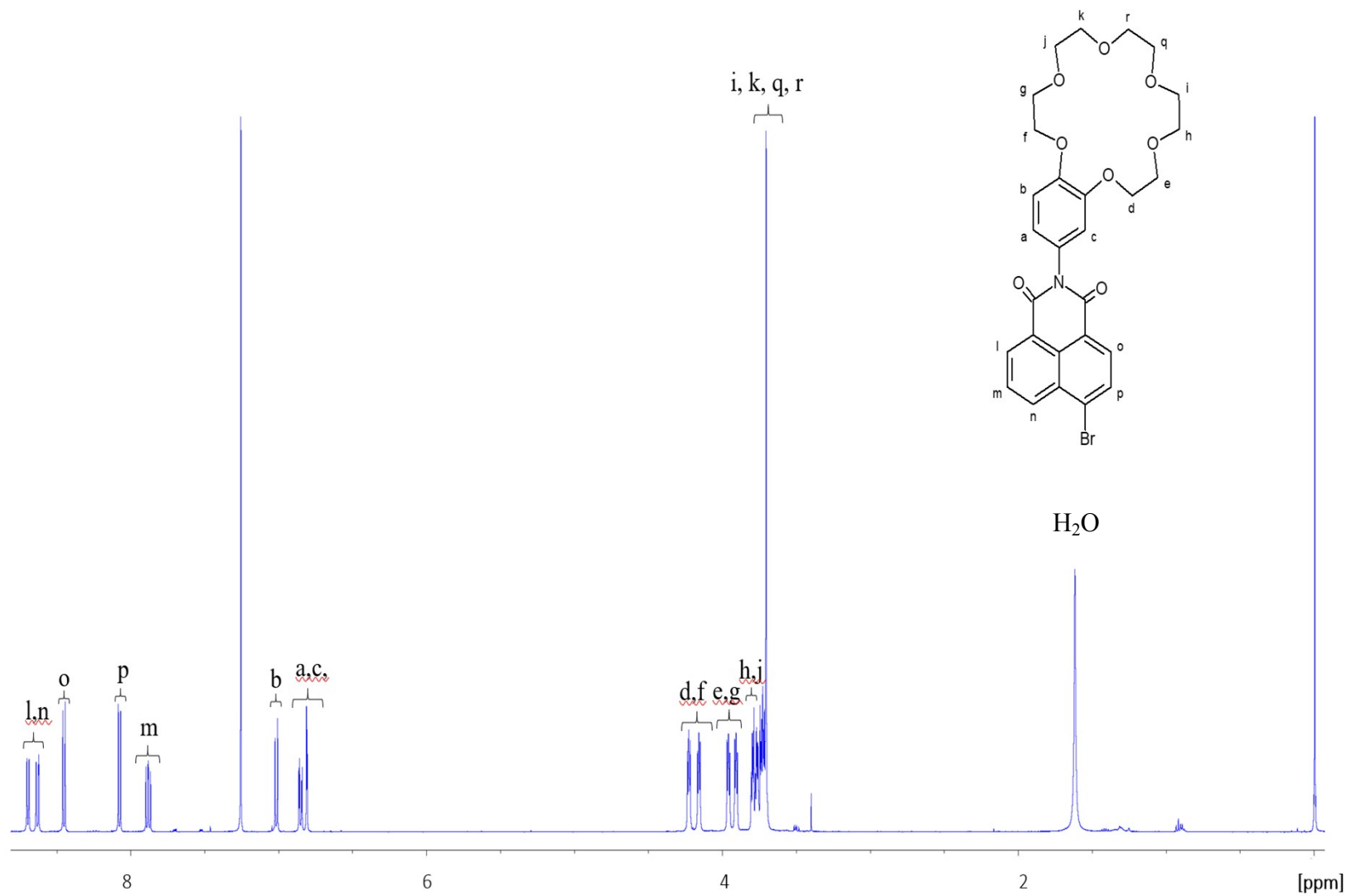


Figure S7. ^1H NMR of **7** in $\text{CDCl}_3/0.03\%$ TMS.

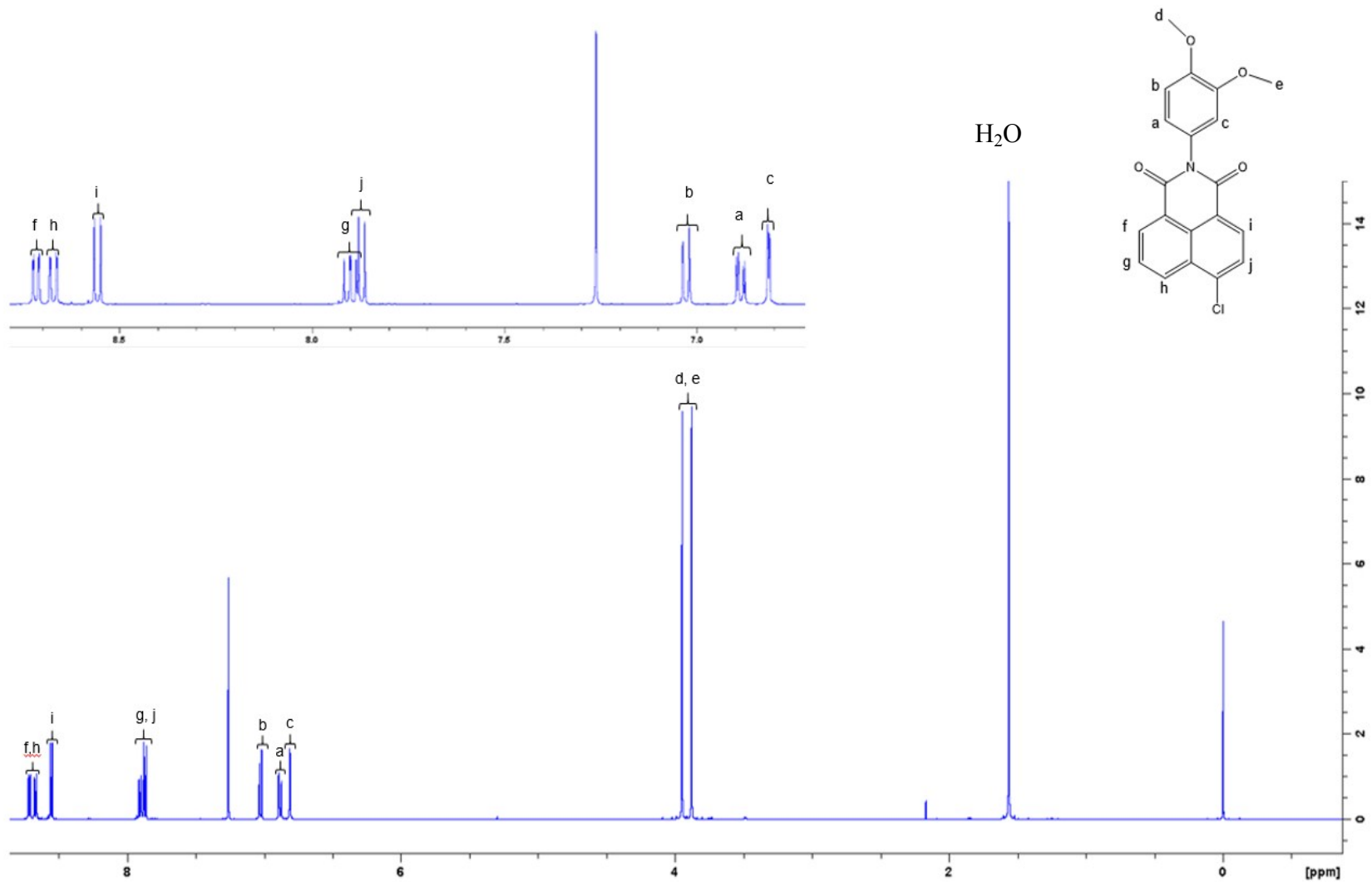


Figure S8. ^1H NMR of **8** in $\text{CDCl}_3/0.03\%$ TMS.

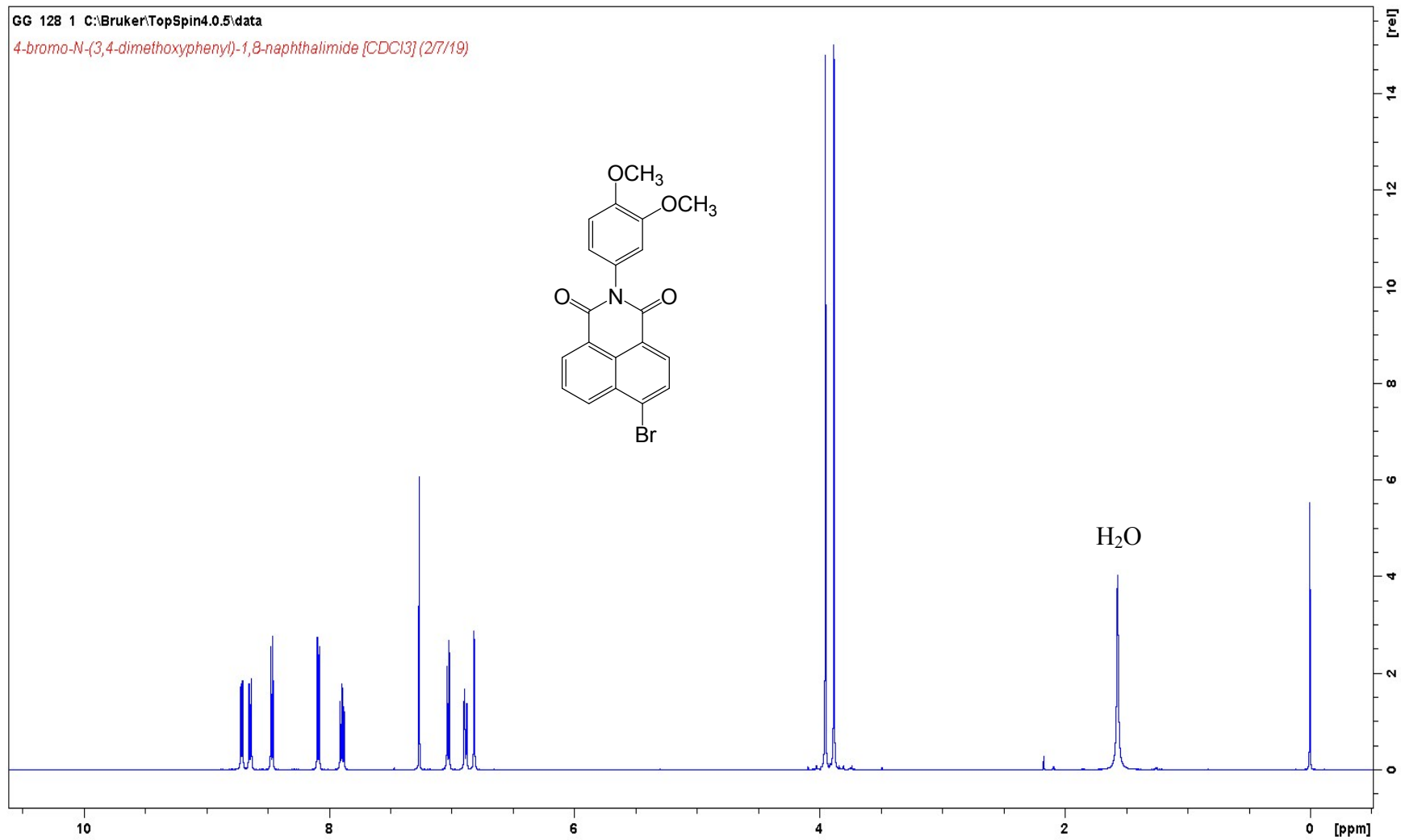


Figure S9. ¹H NMR of **9** in CDCl₃/ 0.03% TMS

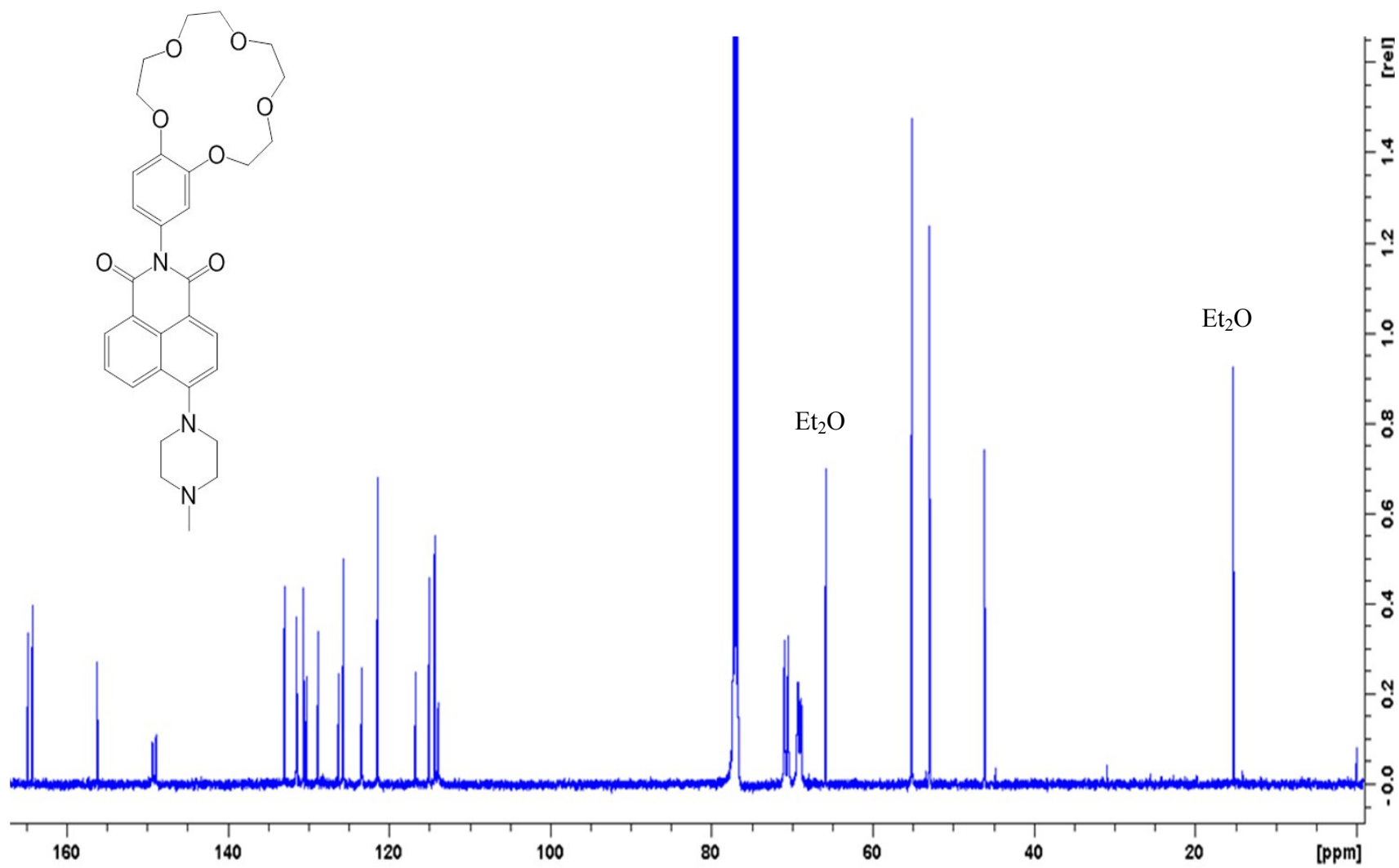


Figure S10. ^{13}C NMR spectrum of **1** in $\text{CDCl}_3/0.03\%$ TMS.

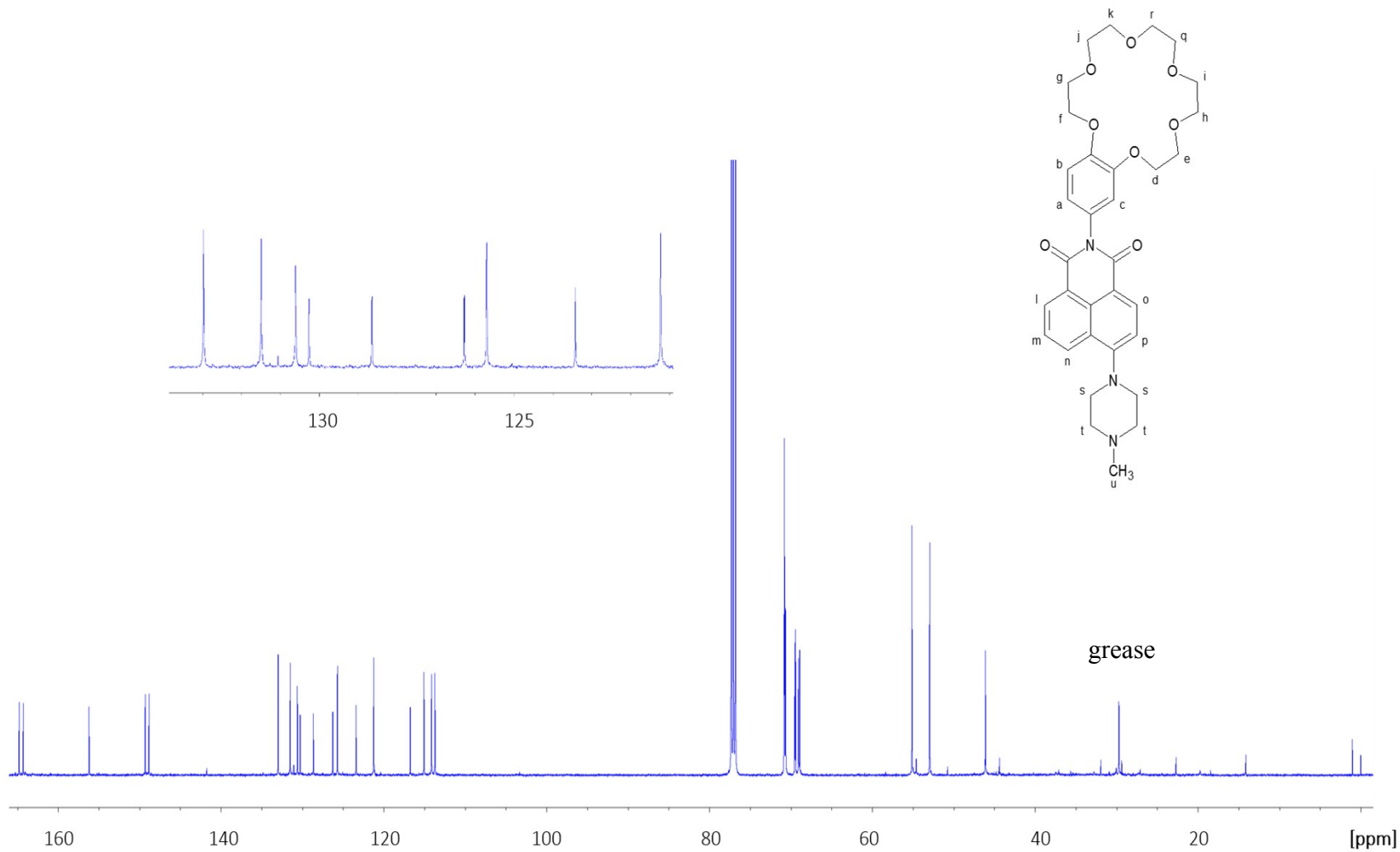


Figure S11. ^{13}C NMR of **2** in $\text{CDCl}_3/0.03\%$ TMS.

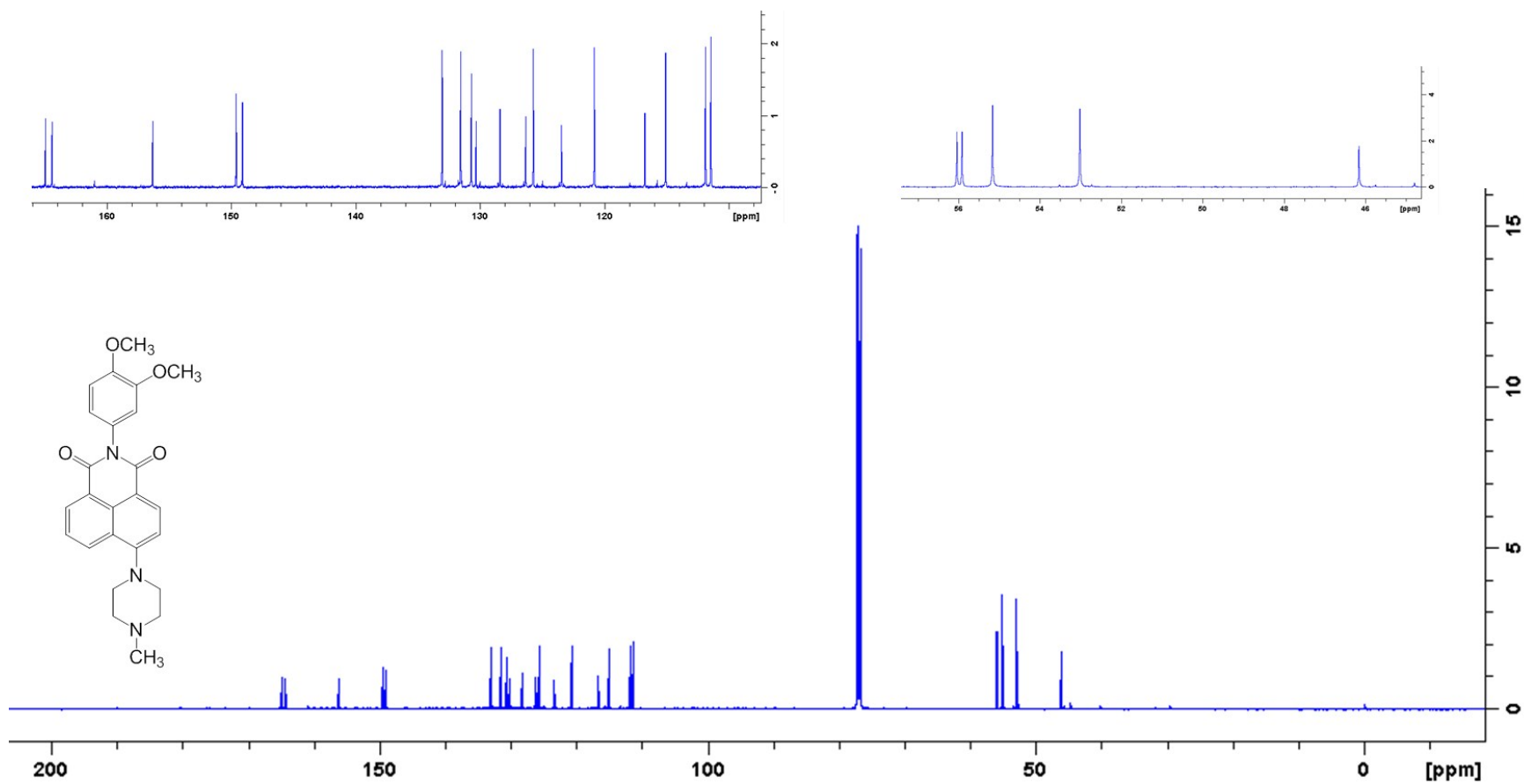


Figure S12. ^{13}C NMR of **3** in $\text{CDCl}_3/0.03\%$ TMS.

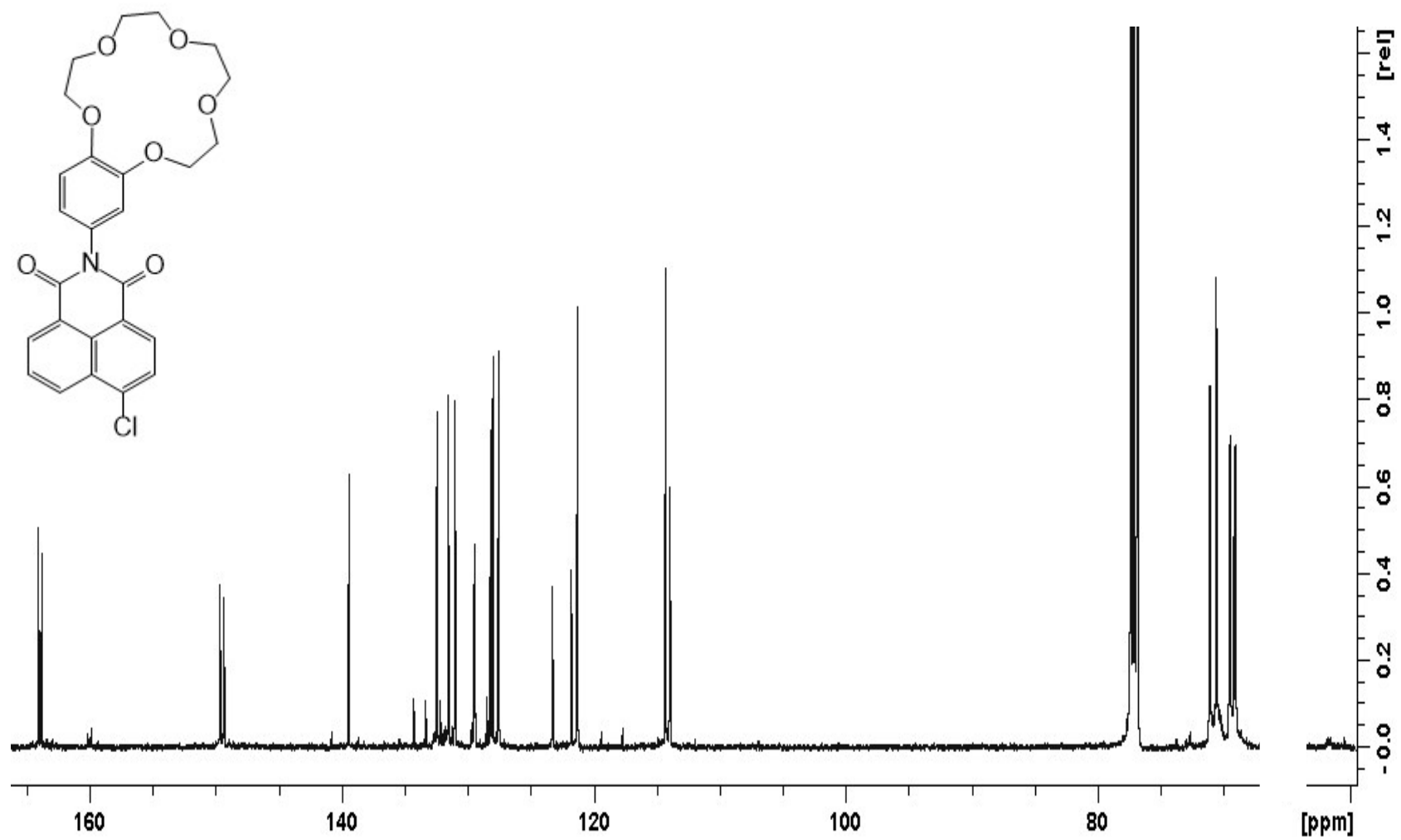


Figure S13. ^{13}C NMR spectrum of **4** in CDCl_3/TMS .

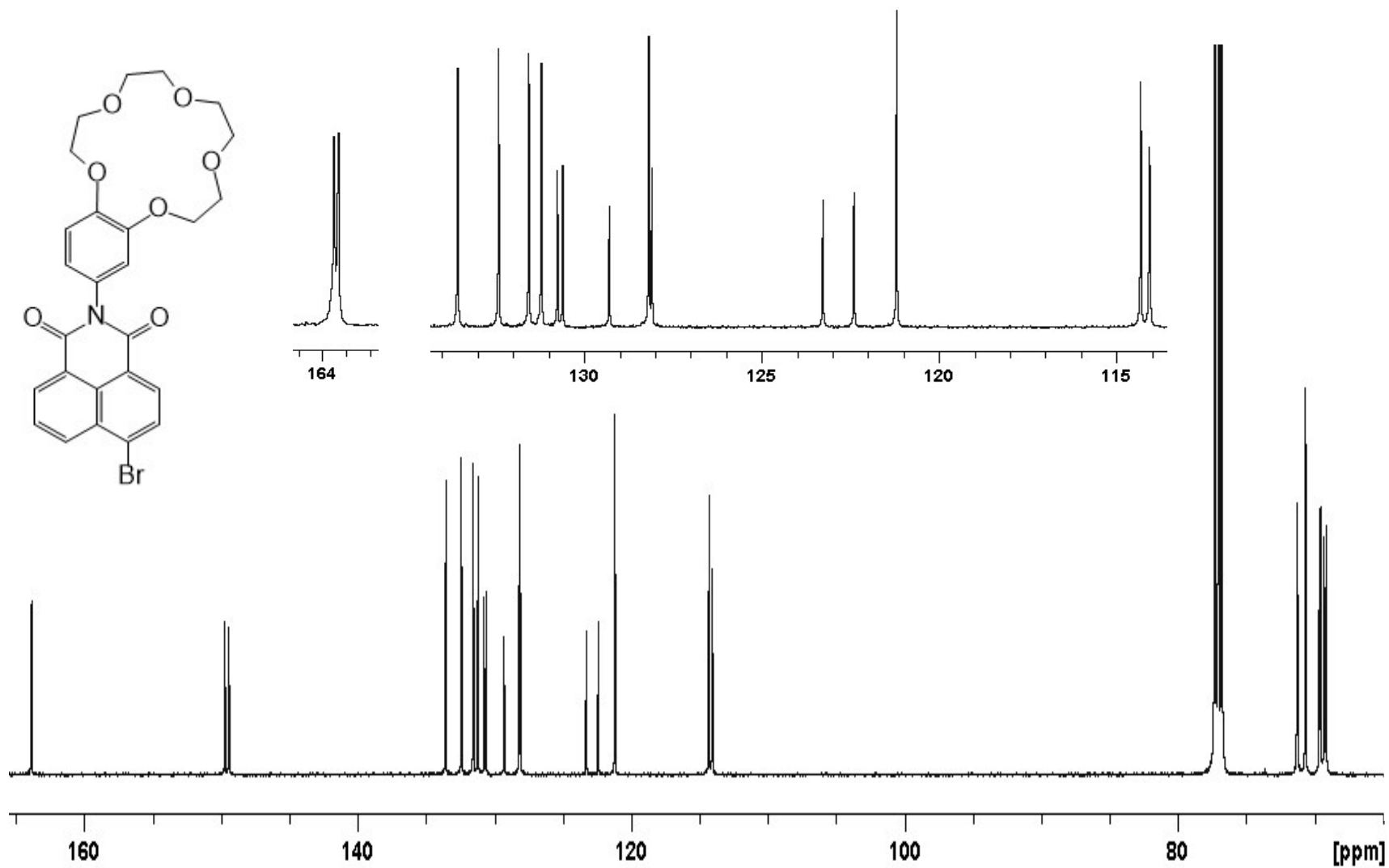


Figure S14. ^{13}C NMR spectrum of **5** in CDCl_3/TMS .

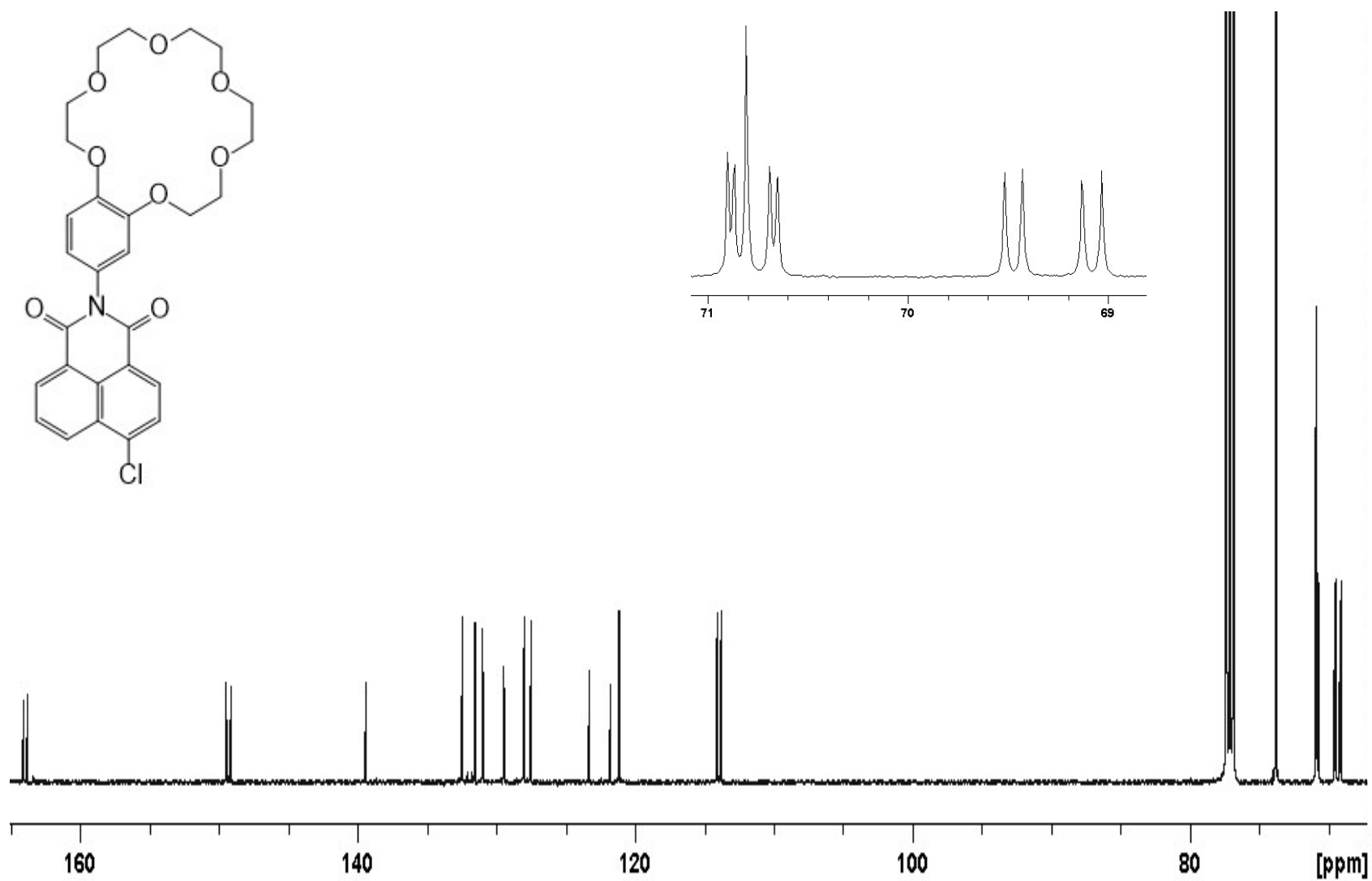


Figure S15. ^{13}C NMR spectrum of **6** in CDCl_3/TMS .

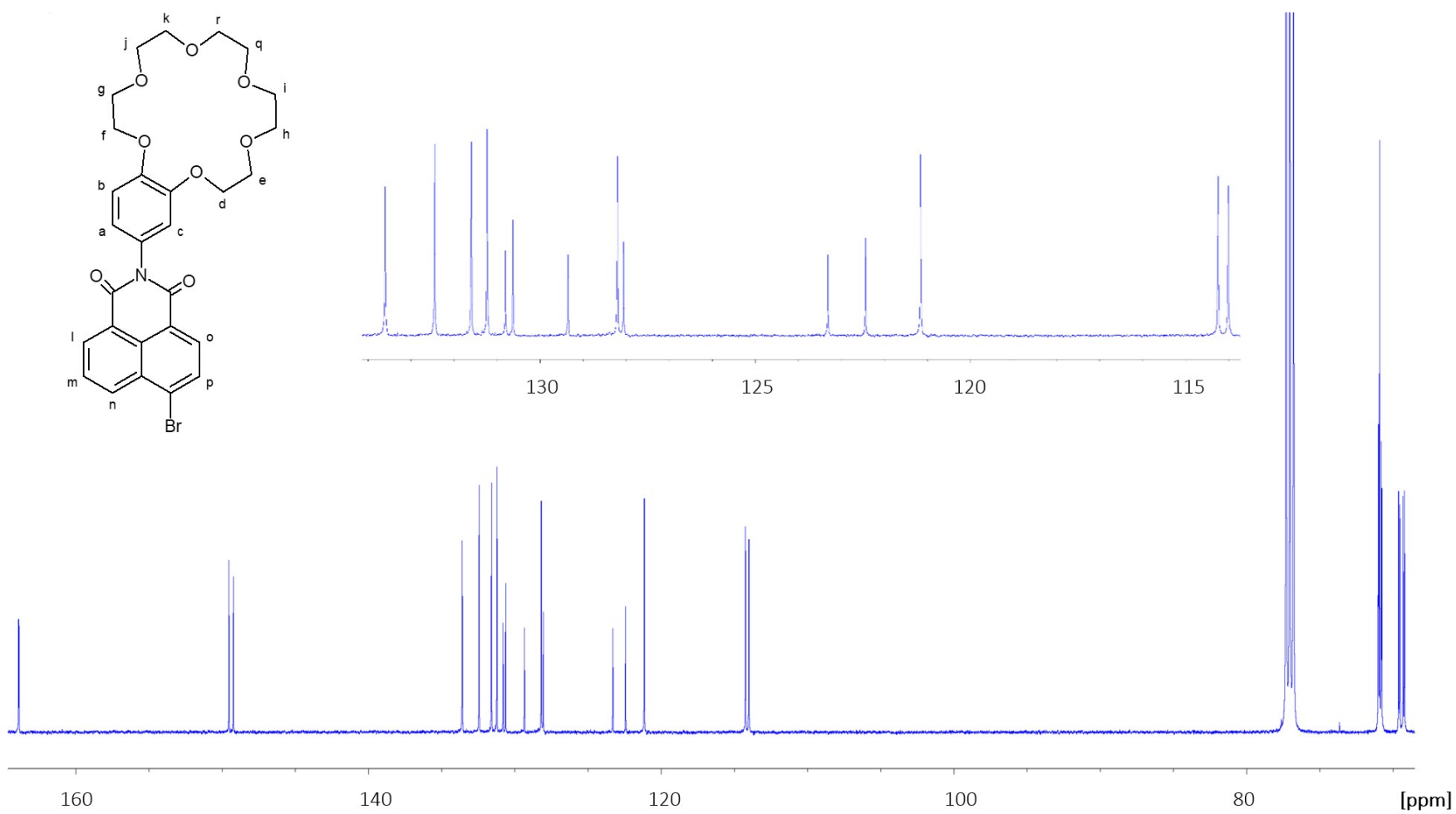


Figure S16. ^{13}C NMR spectrum of 7 in CDCl_3/TMS .

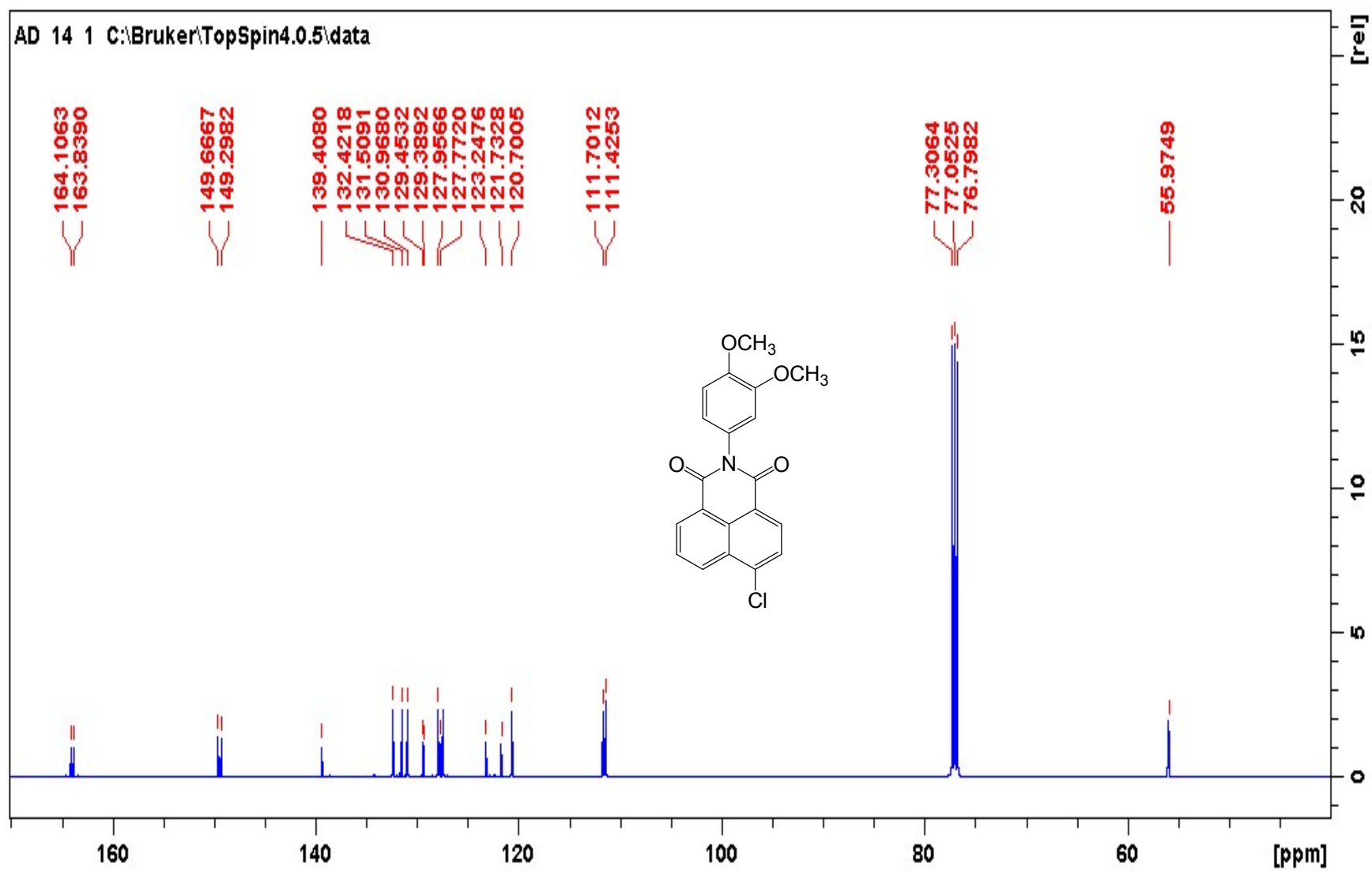


Figure S17. ^{13}C NMR of **8** in CDCl_3 / 0.03% TMS.

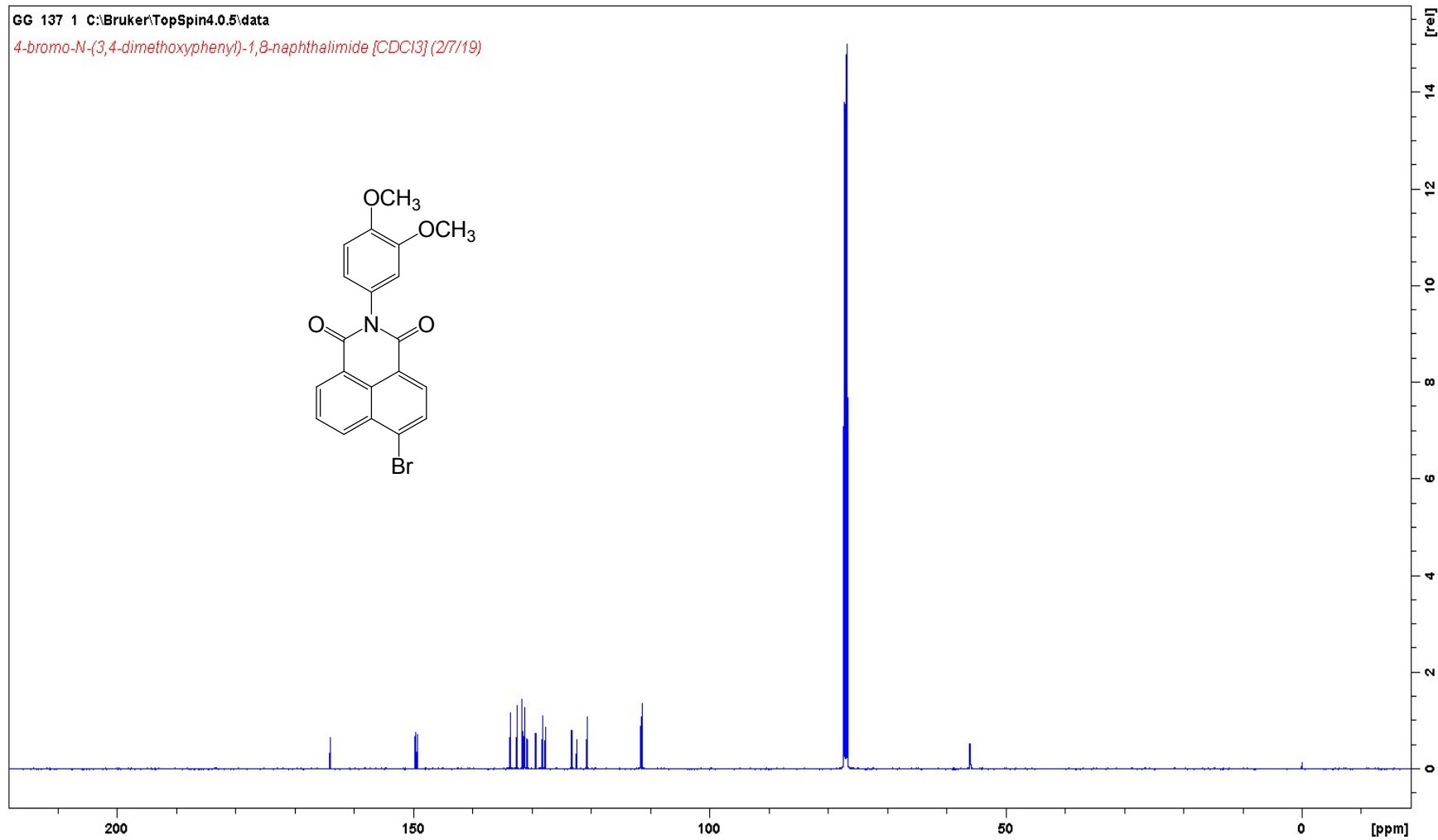


Figure S18. ¹³C NMR of **9** in CDCl₃/ 0.03% TMS.

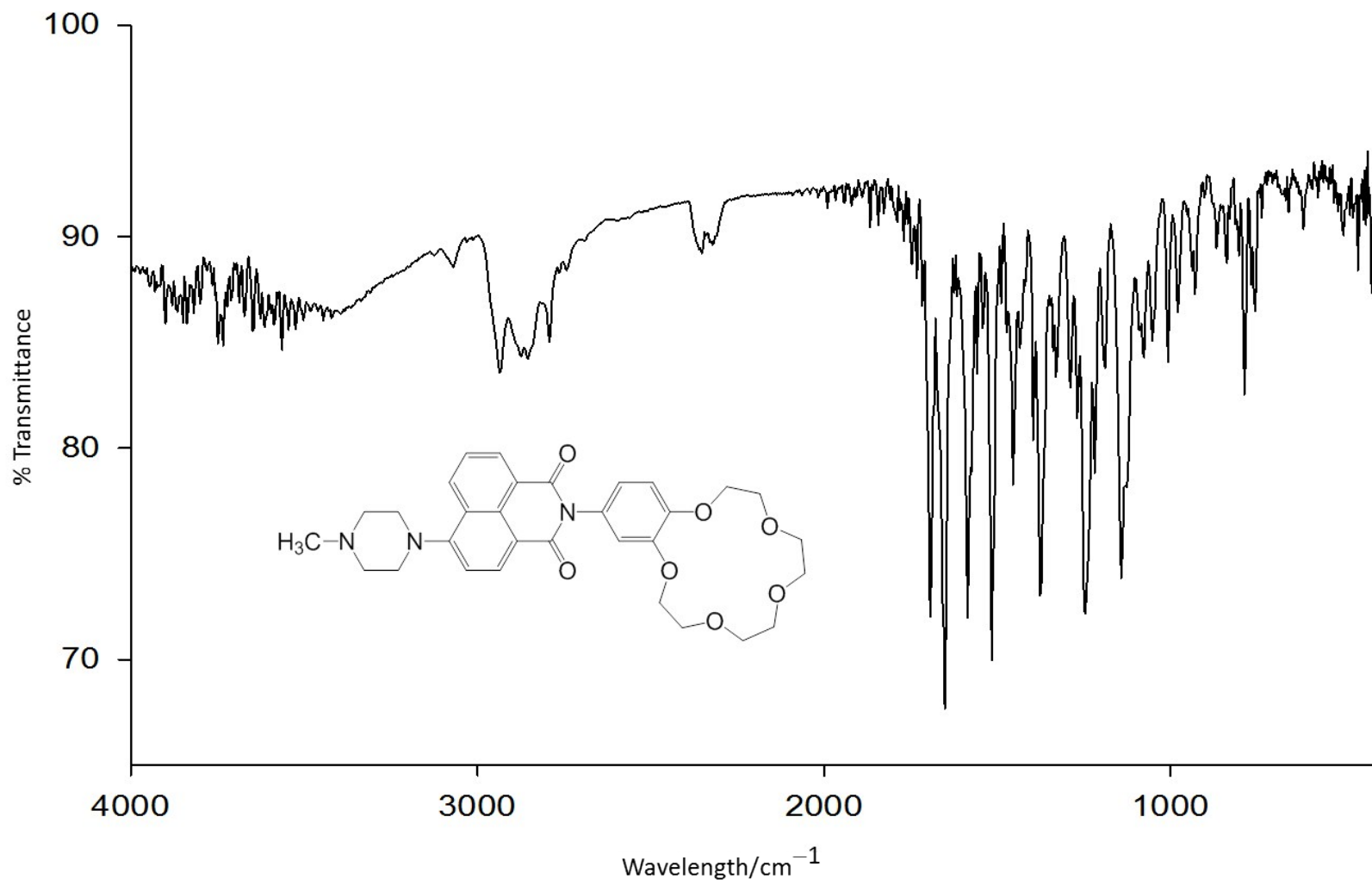


Figure S19. IR spectrum of **1** (KBr disc).

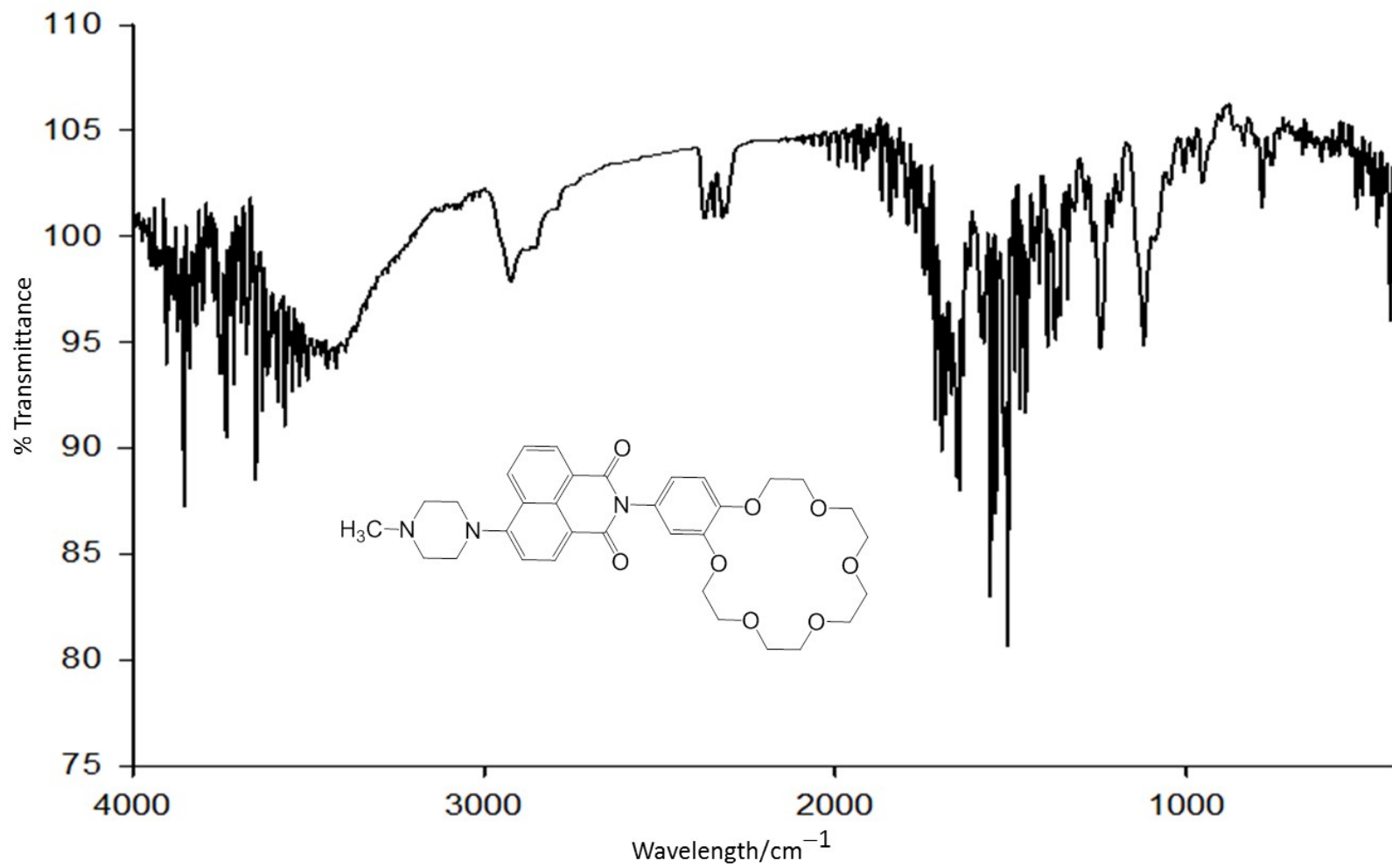


Figure S20. IR spectrum of **2** (KBr disc).

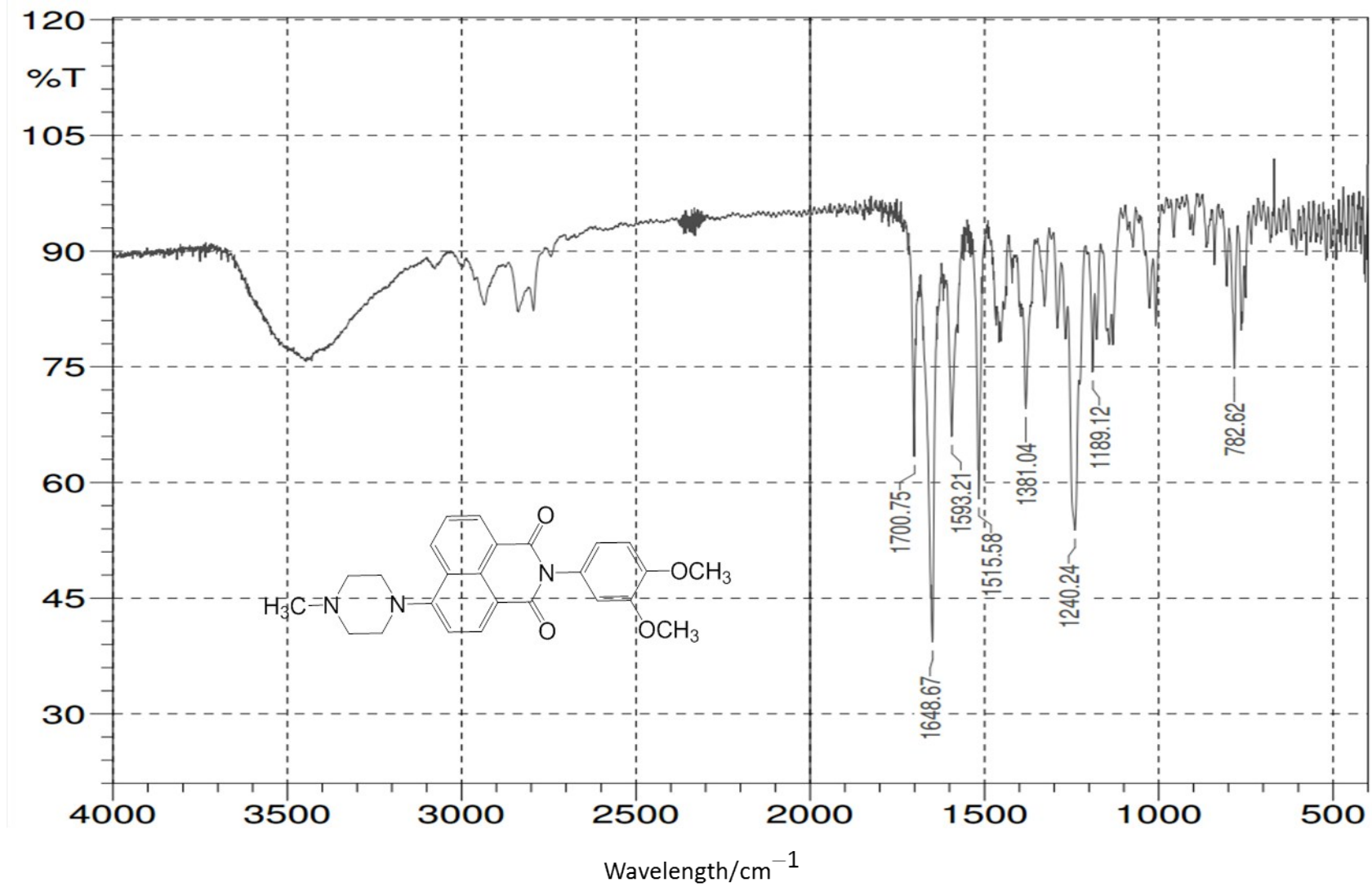


Figure S21. IR spectrum of 3 (KBr disc).

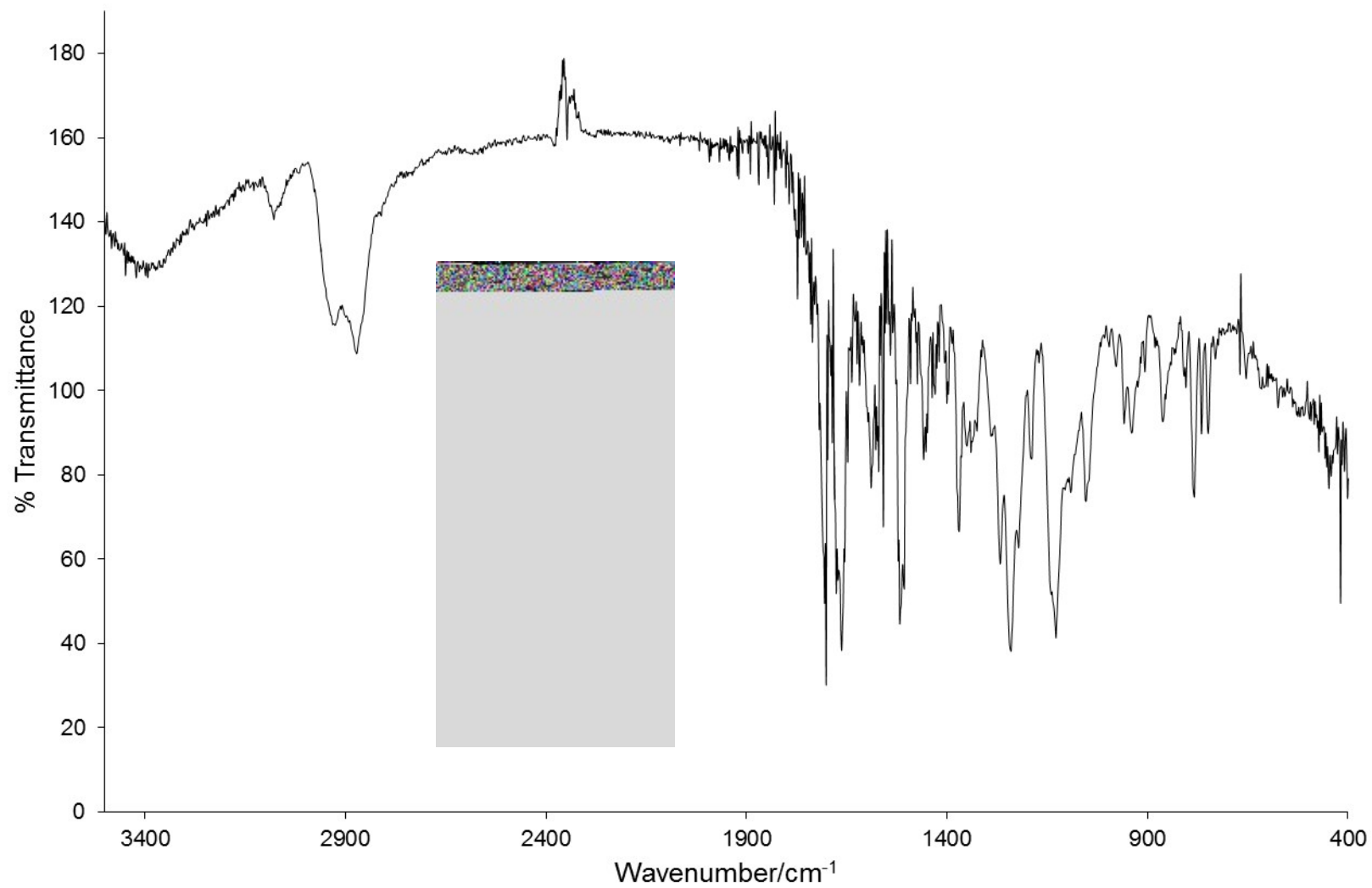


Figure S22. IR spectrum of 4 (KBr disc).

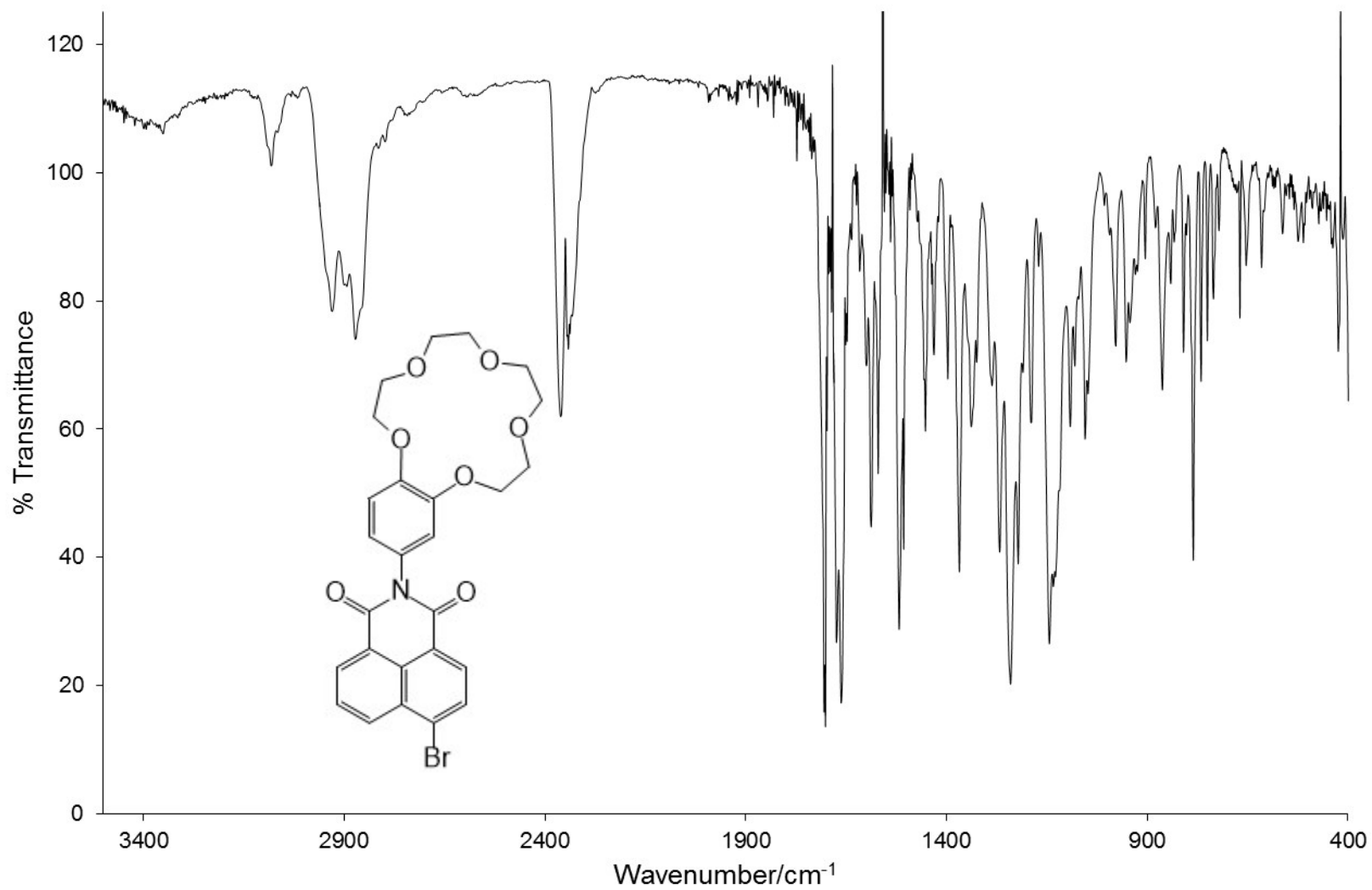


Figure S23. IR spectrum of **5** (KBr disc).

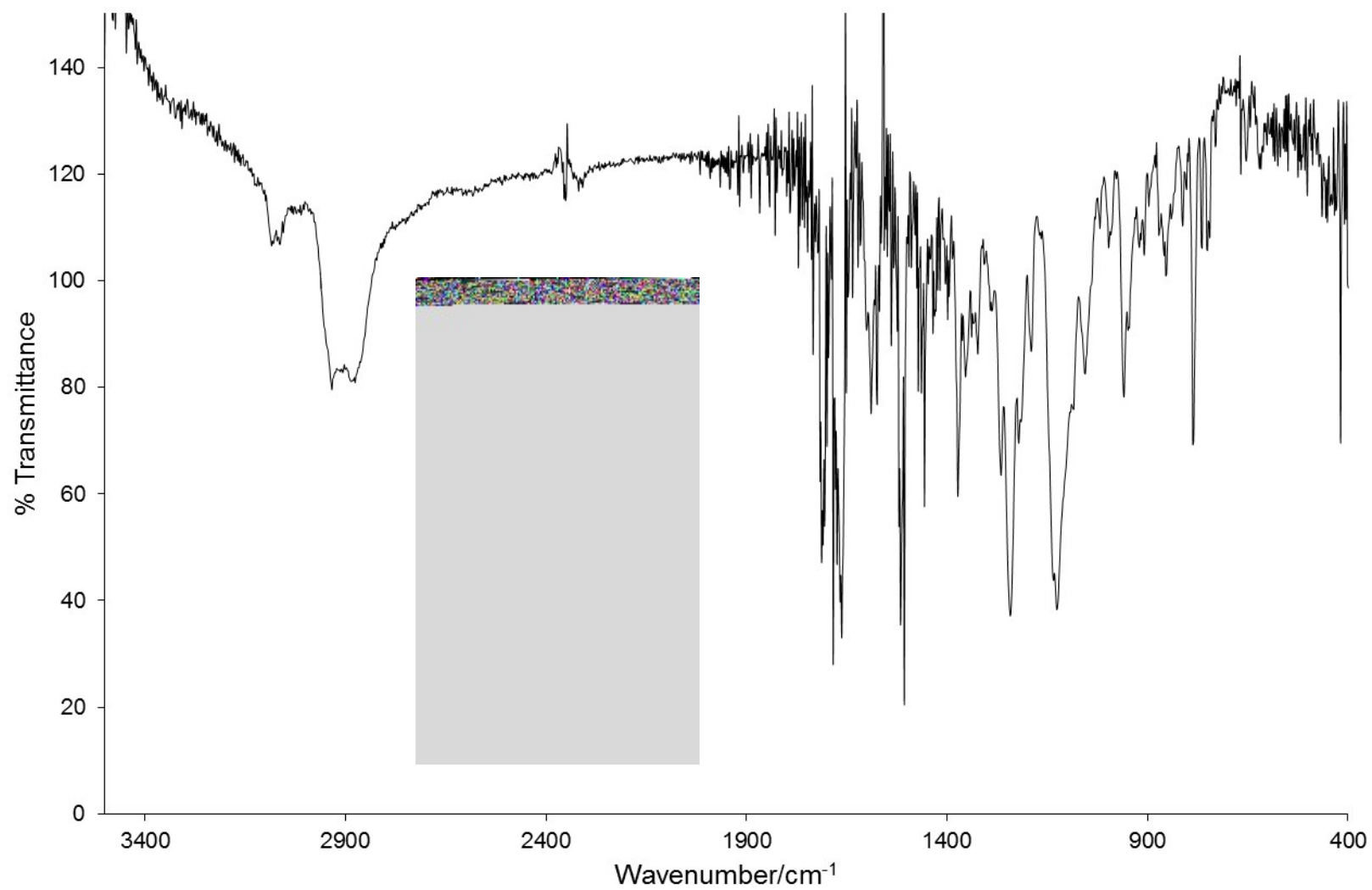


Figure S24. IR spectrum of **6** (KBr disc).

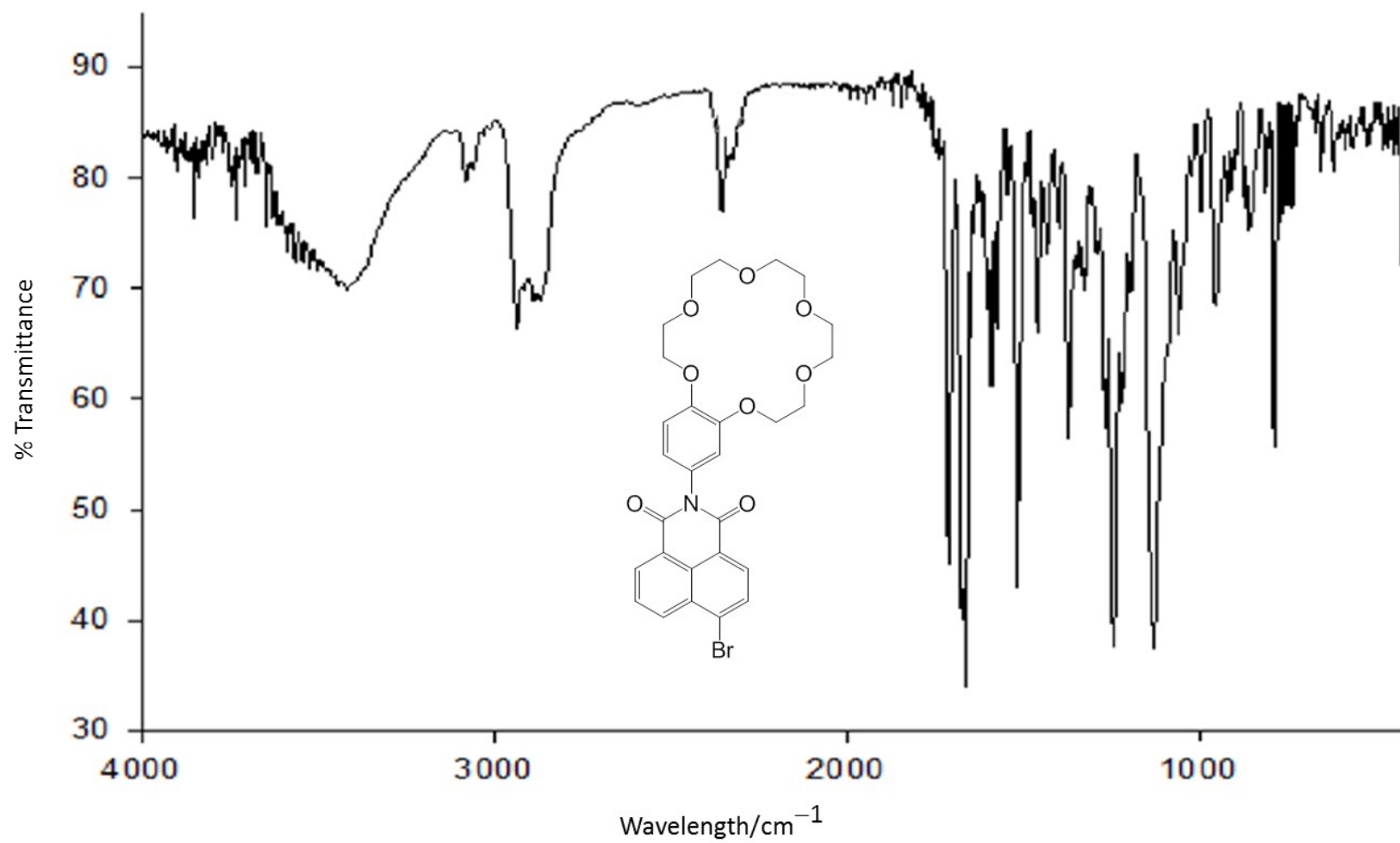


Figure S25. IR spectrum of 7 (KBr disc).

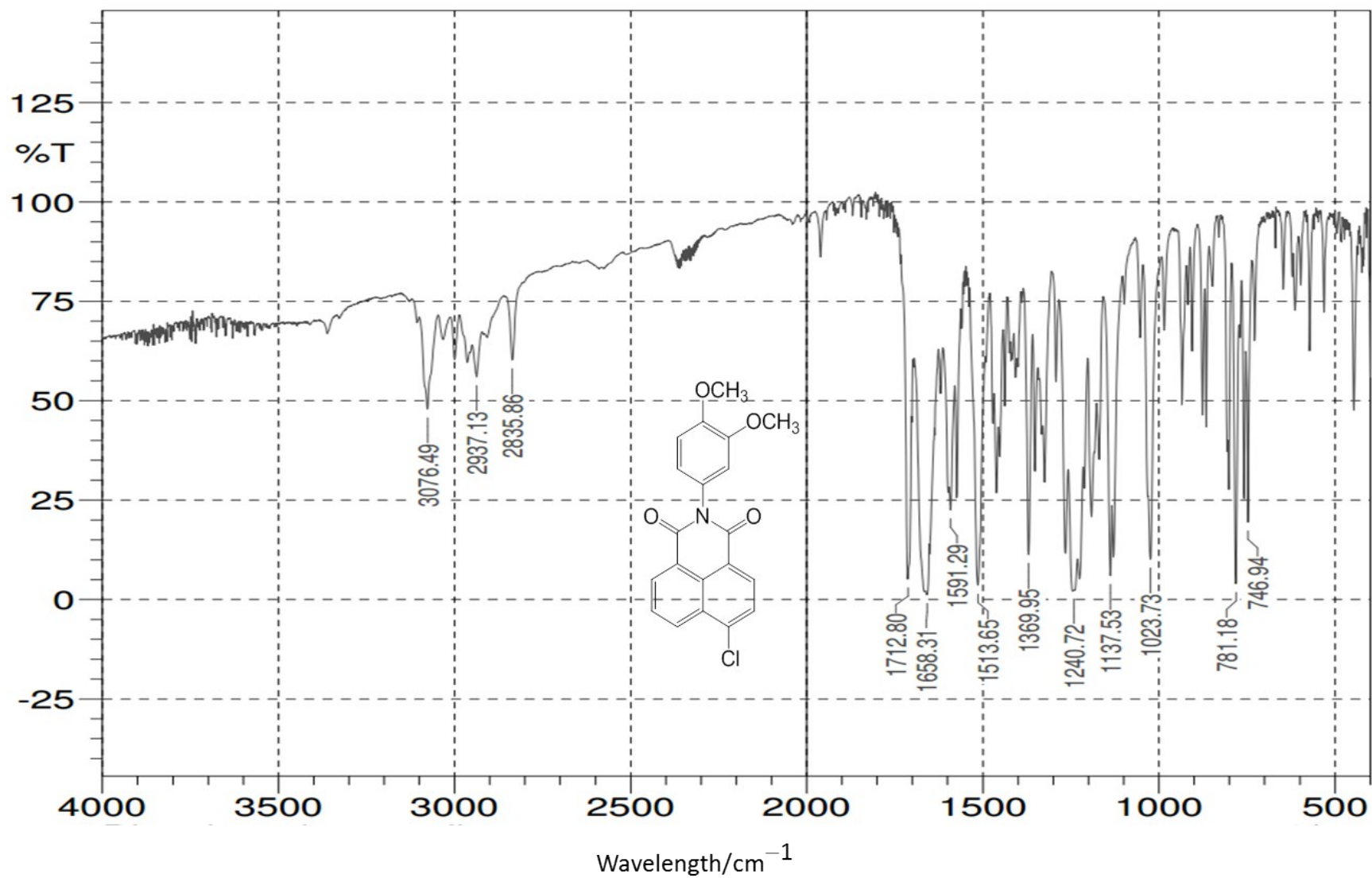


Figure S26. IR spectrum of **8** (KBr disc).

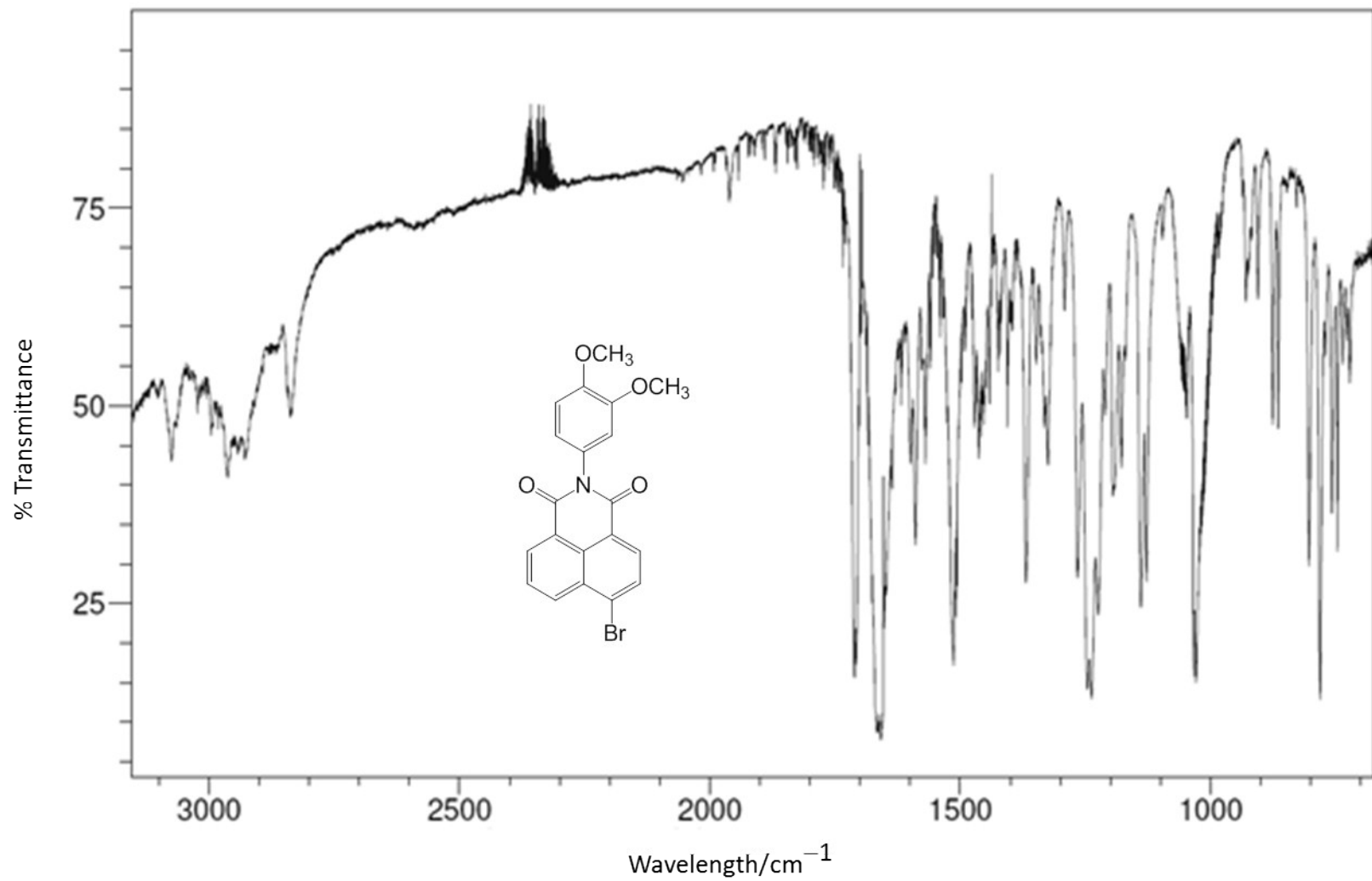


Figure S27. IR spectrum of **9** (KBr disc).

CNMP_M1
MEDAC_CNMP_M1 8 (0.254) Cm (8-35:56)

ES-ToF

27-May-2016
1: TOF MS ES+
2.07e3

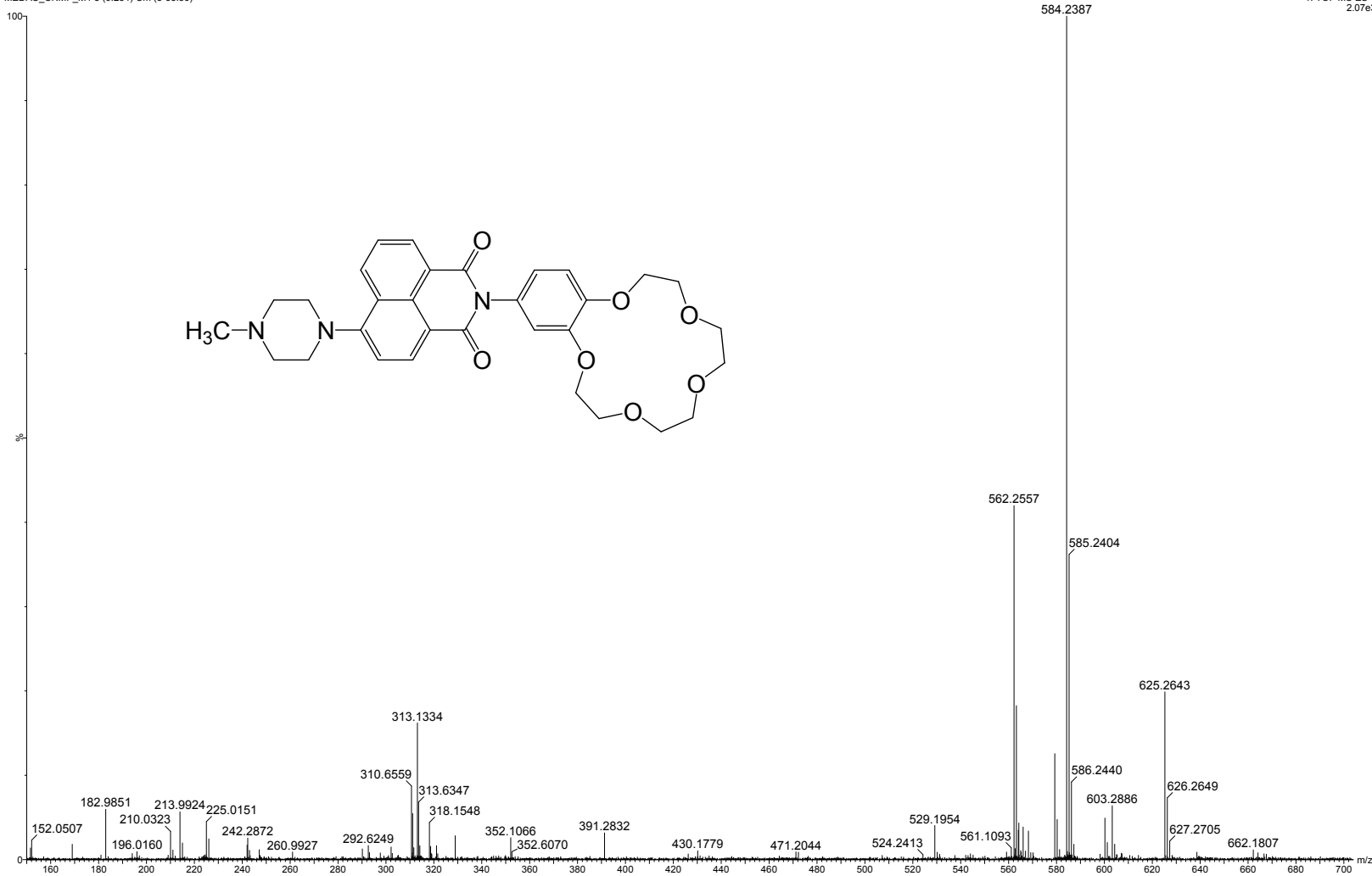


Figure S28. HRMS of compound 1.

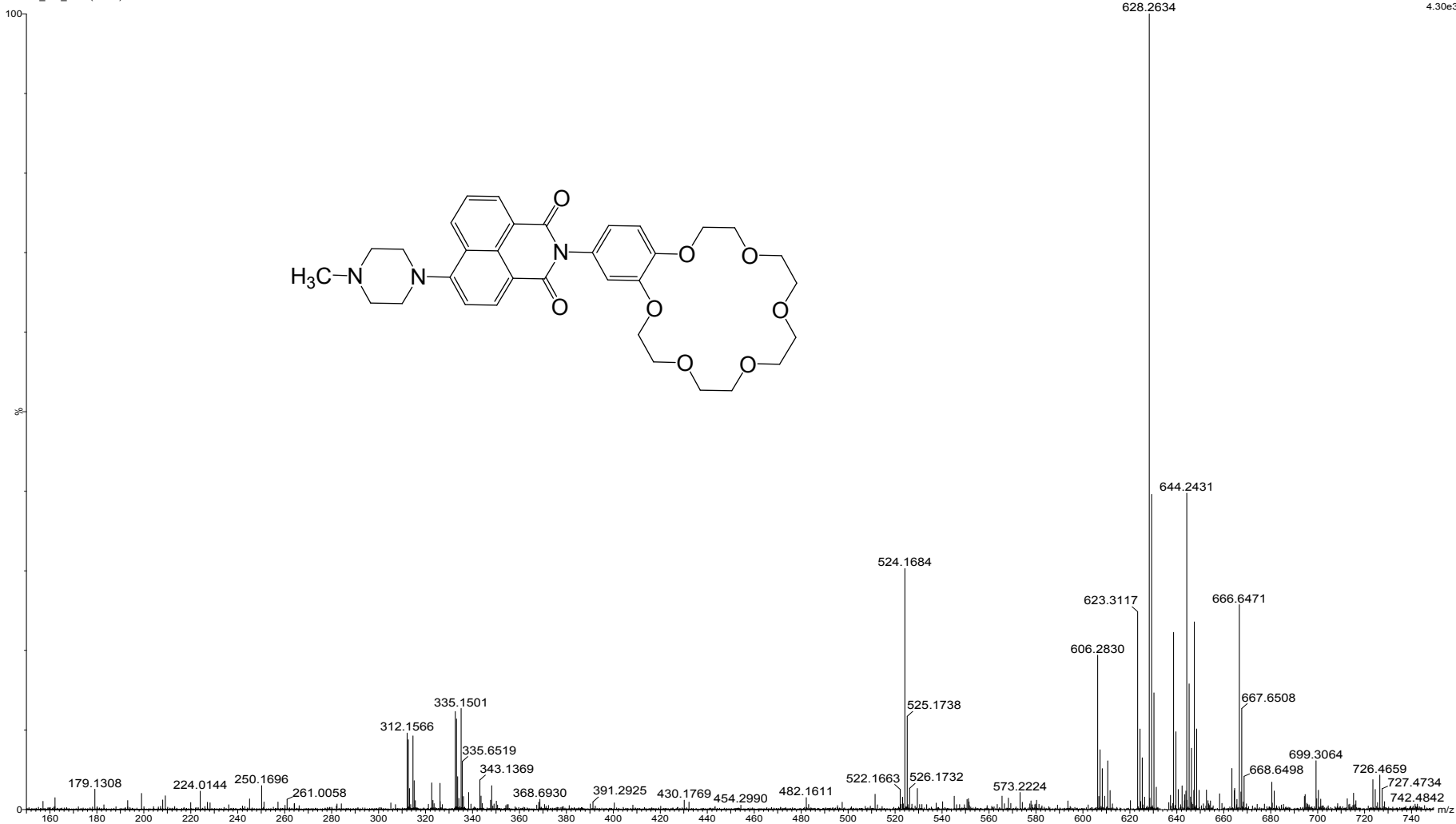


Figure S29. HRMS of compound 2.

MEDAC_AD_DMN
MEDAC_AD_DMN 6 (0.199)

19-Jul-2019
1: TOF MS ES+
298

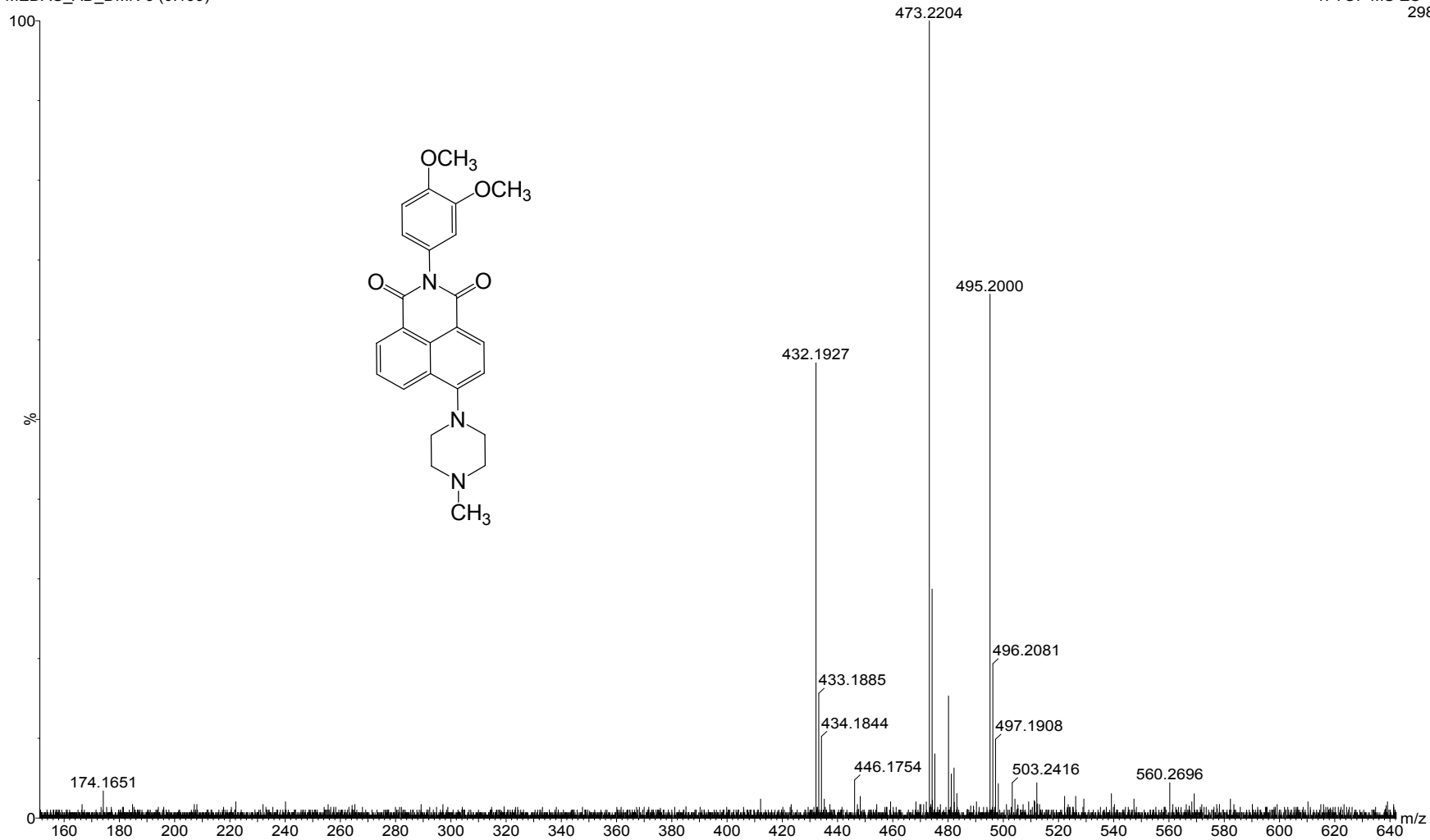


Figure S30. HRMS of compound 3.

MEDAC_GAMS1
MEDAC_GAMS1 11 (0.367)

ES-ToF

12-May-2017
1: TOF MS ES+
2.82e3

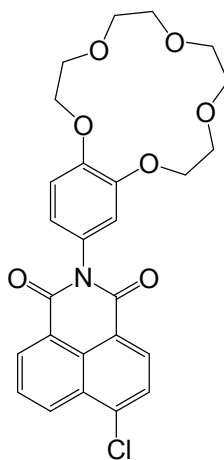
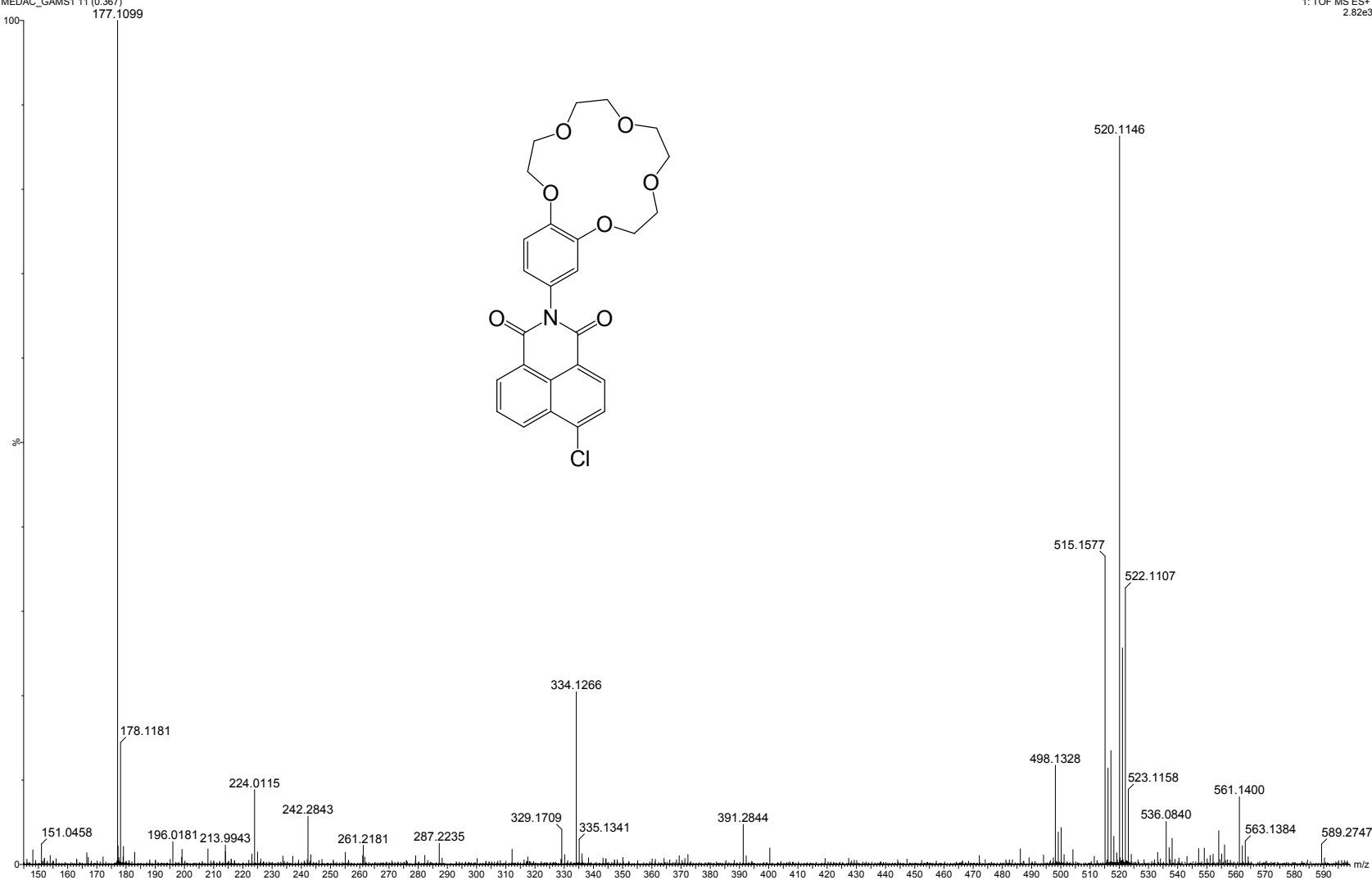


Figure S31. HRMS of compound 4.

MEDAC_GAMS2
MEDAC_GAMS2 10 (0.340)

ES-ToF

12-May-2017
1: TOF MS ES+
2.81e3

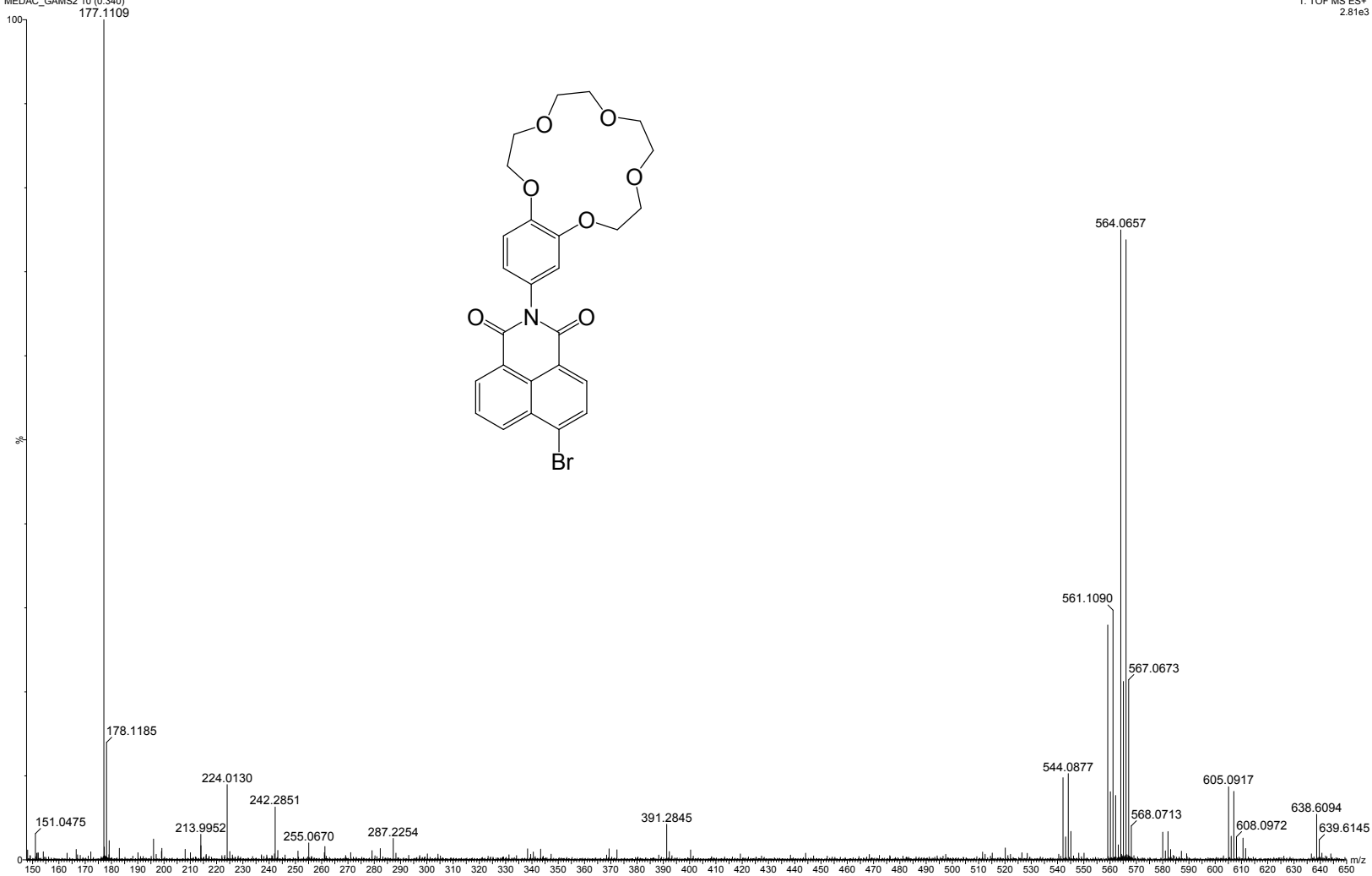


Figure S32. HRMS of compound 5.

MEDAC_GAMS3
MEDAC_GAMS3 6 (0.199)

ES-ToF

12-May-2017
1: TOF MS ES+
3.95e4

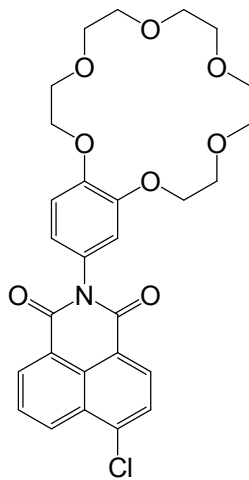
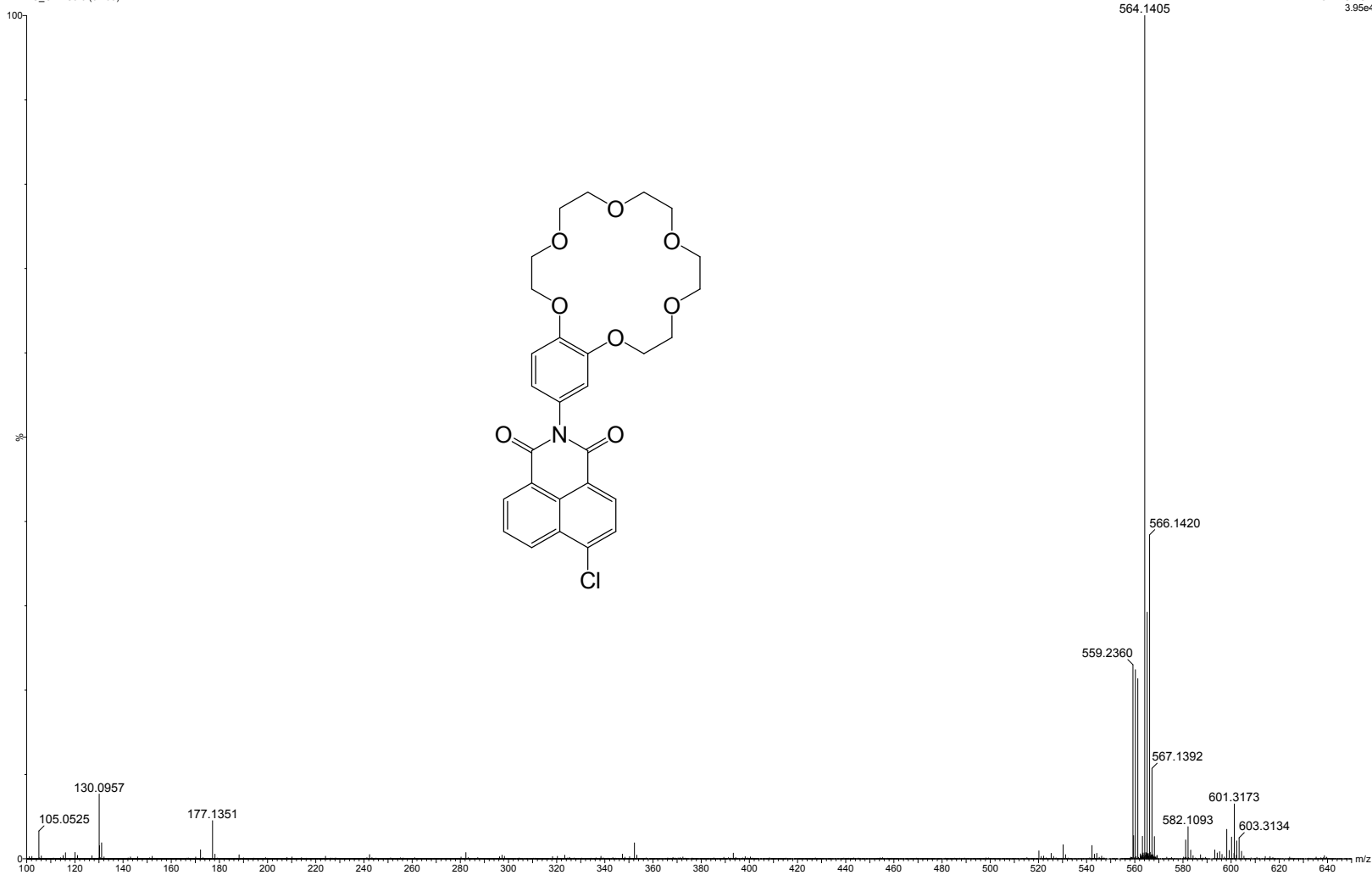


Figure S33. HRMS of compound 6.

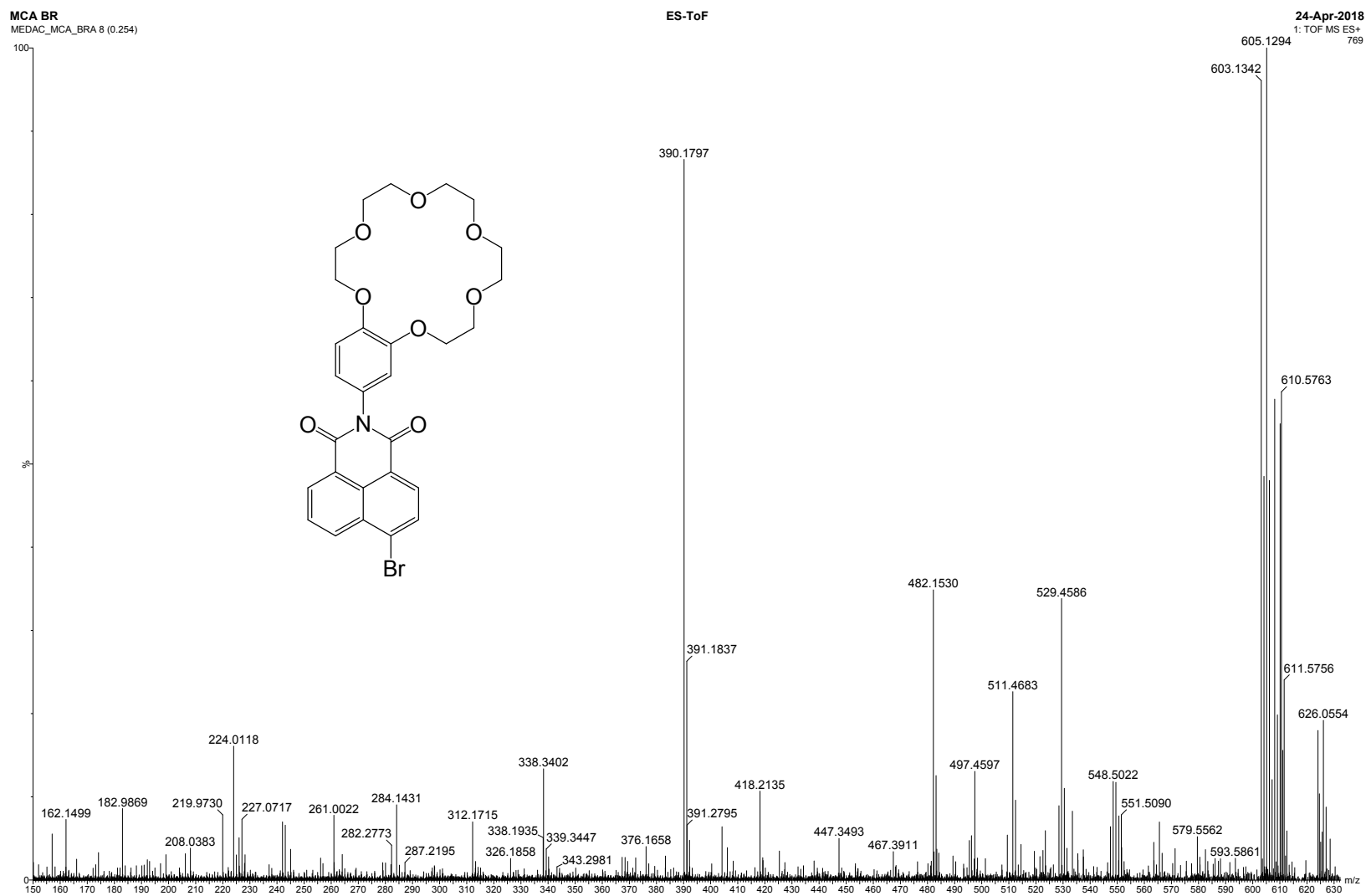


Figure S34. HRMS of compound 7.

MEDAC_AD08
MEDAC_AD08 8 (0.255)

18-Dec-2019
1: TOF MS ES+
424



Figure S35. HRMS of compound 8.

MEDAC_GG2
MEDAC_GG2 8 (0.254)

19-Jul-2019
1: TOF MS ES+
297

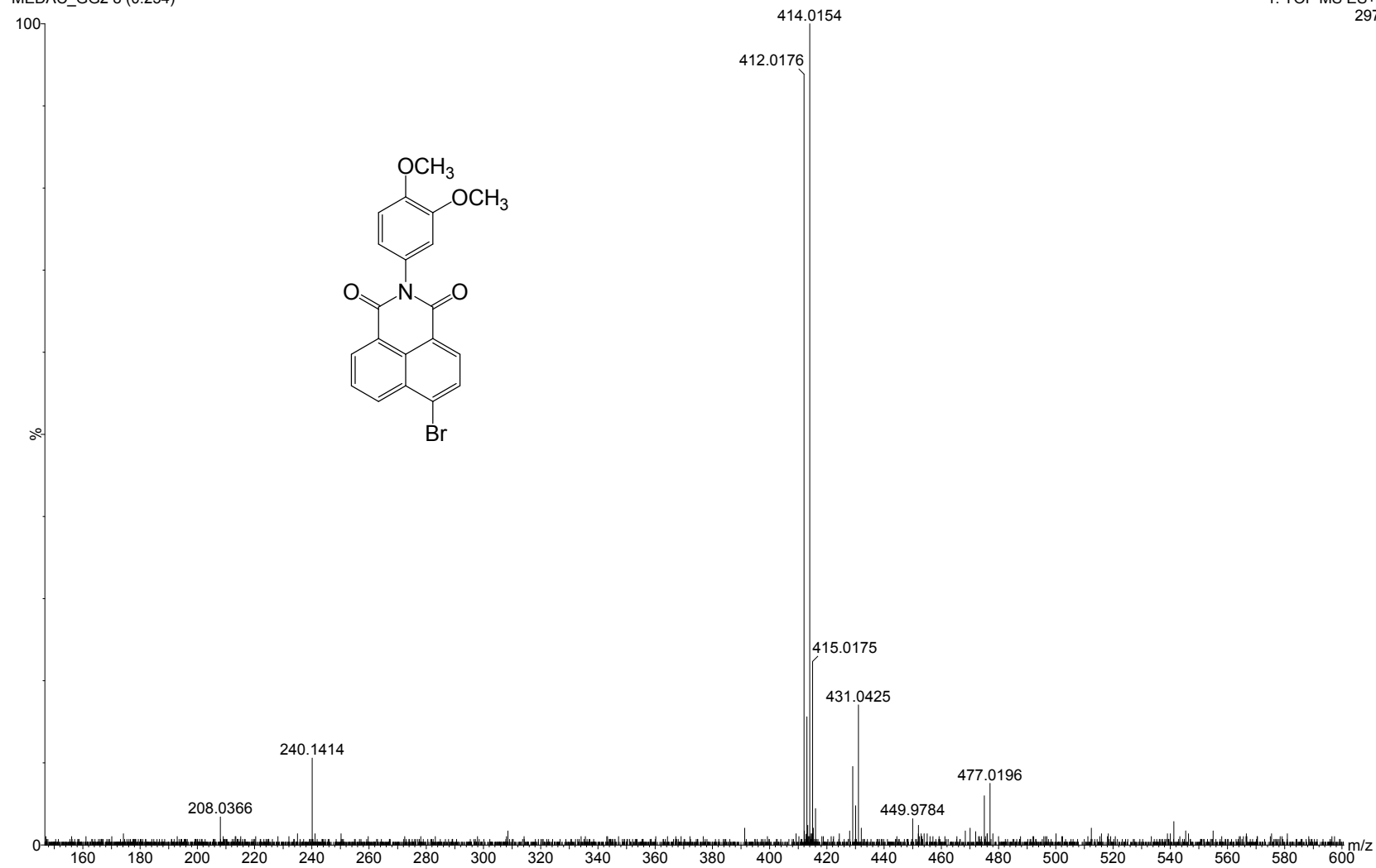


Figure S36. HRMS of compound 9.